



Mapping Middle Stone Age human mobility in the Makgadikgadi Pans (Botswana) through multi-site geochemical provenancing of silcrete artefacts

David J. Nash^{a, b, *}, T. Jake R. Ciborowski^a, Sheila D. Coulson^c, Sigrid Staurset^d, Sallie L. Burroughs^d, Sarah Mothulatshipi^e, David S.G. Thomas^{b, d}

^a School of Applied Sciences, University of Brighton, Lewes Road, Brighton, BN2 4GJ, United Kingdom

^b School of Geography, Archaeology and Environmental Studies, University of the Witwatersrand, South Africa

^c Institute of Archaeology, Conservation and History, University of Oslo, Blindernveien 11, 0315, Oslo, Norway

^d School of Geography and the Environment, University of Oxford, South Parks Road, Oxford, OX1 3QY, United Kingdom

^e Department of History, University of Botswana, Private Bag UB, 0022, Gaborone, Botswana

ARTICLE INFO

Article history:

Received 19 April 2022

Received in revised form

1 August 2022

Accepted 22 August 2022

Available online 31 October 2022

Keywords:

Raw material procurement

Silcrete provenancing

Middle Stone Age

Human mobility

Lithic technology

Chaîne opératoire

ABSTRACT

Analyses of the distance over which lithic raw materials were transported for use in stone tool production provide important insights into early human mobility through prehistoric landscapes. This study combines the use of geochemical provenancing, *chaîne opératoire* analysis and geochronology to examine patterns of lithic raw material procurement at five single-use open-air Middle Stone Age (MSA) archaeological sites in Ntswetwe Pan, part of the Makgadikgadi Pans complex in north-central Botswana. Maximum ages of the five sites ranged from 106 ± 3 to 69 ± 7 ka, with site formation thought to have occurred before and after a lake high stand dated to c. 72–57 ka. Tool manufacture at all sites was largely confined to the production of MSA points, with silcrete used exclusively as the raw material. Geochemical provenancing investigations aimed to identify the specific silcrete outcrops used as lithic raw material sources. Analysis of contemporary pan floor deposits show that sediment (and hence silcrete) geochemistry in Ntswetwe is determined by the proportional sediment input into the pan from fluvial systems with different catchment geologies. Immobile trace element signatures for 46 waste manufacturing flakes were compared against equivalent data for 321 silcrete samples collected at outcrops within and beyond Ntswetwe Pan. Waste flakes were chosen to be representative of the main silcrete raw material types present within the artefact assemblage at each site. Fifteen waste flakes were shown to match specific outcrops on the basis of their geochemical signatures and petrographic properties; all matching outcrops were within Ntswetwe Pan, at distances ranging from 7 to 55 km from individual sites. Multi-site analysis of procurement patterns identifies common silcrete source areas, revealing a preference for silcrete from particular locations within Ntswetwe Pan. Given that the five archaeological sites were likely occupied at different times, this resource preference may have been a longer-term behavioural feature of MSA populations in the Ntswetwe region. The distances over which silcrete was transported in Ntswetwe Pan are smaller than identified in investigations at similar-aged MSA sites in northwest Botswana. The reasons for the different silcrete procurement ranges in the two regions are likely related to silcrete availability and/or raw material preference, but this requires further investigation.

© 2022 The Authors. Published by Elsevier Ltd. This is an open access article under the CC BY license (<http://creativecommons.org/licenses/by/4.0/>).

1. Introduction

Studies of the distance over which lithic raw materials were transported for use in stone tool manufacture are crucial for our understanding of early human mobility through prehistoric landscapes. The physical location, quality and accessibility of lithic raw

* Corresponding author. School of Applied Sciences, University of Brighton, Lewes Road, Brighton, BN2 4GJ, United Kingdom.

E-mail address: d.j.nash@brighton.ac.uk (D.J. Nash).

material sources shape the fundamental framework of resource availability and hence the distance over which stone needed to be transported (e.g. Andrefsky, 1994; Minichillo, 2006; Brooks et al., 2018; Kot et al., 2020; Will, 2021). Resource availability can, however, change over time as, for example, raw material sources are worked out or sources in low-lying landscape positions (e.g. adjacent to rivers or lakes) become either inaccessible or exposed following hydroclimatic shifts (see Nash et al., 2016). Socioeconomic factors are also likely to have influenced how far, and to where, our ancestors travelled to obtain raw materials. Carrying stone requires energy expenditure and so influences (i) the production stage at which artefacts are transported, and (ii) rates of tool use/discard and curation/recycling (e.g. Ambrose, 2006; Thompson et al., 2010; Porraz et al., 2013; Wilkins, 2017; Will and Conard, 2020). Factors such as the capacity for in-depth planning, communication and the potential for commodity exchange between groups may also affect the choice of raw materials transported and their variation, as knowing that suitable stone is available in an area (through direct or indirect means) may lessen the need for transport from elsewhere (e.g. Meltzer, 1989; Merrick et al., 1994; Ambrose, 2006; McCall, 2007; Brown, 2011; Aubry et al., 2012; Porraz et al., 2013; Wilkins, 2017). Foraging strategies, group mobility and seasonal cycles of human movement through landscapes affect both the geography of raw material procurement and who is involved in that procurement (e.g. Bamforth, 1991; Nelson, 1991; Andrefsky, 1994; Kot et al., 2020). Indications of territoriality may also be inferred from the use or choice of specific raw material sources and site-to-source distances (e.g. Ambrose, 2012; Eren et al., 2013; Mackay et al., 2022).

The most accurate means of determining the source areas of material used in lithic production is through geochemical provenancing. Various stone types have been investigated in provenancing studies, most notably obsidian, chert, flint, dolerite, quartzite, and, in the last decade, silcrete (e.g. Cochran et al., 2017; Kurpiel et al., 2019). When information from provenancing studies is combined with lithic analyses it becomes possible to gain insights into time-specific resource procurement and transport strategies. Geochemical provenancing of silcrete raw materials at White Paintings Shelter (northwest Botswana), for example, revealed long-distance transport of silcrete to the rock shelter during the Middle Stone Age (MSA), with silcrete sources 220–295 km distant preferred over much closer outcrops (Nash et al., 2013). The in-depth “reading” of lithics from the site using a *chaîne opératoire* approach (whereby refitting is used to identify the reduction strategies employed at each stage of tool manufacture, as well as post-production modifications; see Pelegrin, 1990) further showed that long-distance transport was used throughout the 3 m MSA sequence (Nash et al., 2013). Application of the same combined approach at three nearby MSA sites (Rhino Cave, Corner Cave, ≠Gi) suggests that this stone procurement strategy was a repeated and extensively used behaviour in this part of the Middle Kalahari (Nash et al., 2016). Silcrete artefacts were brought to the sites at various stages of the tool production cycle and, with the exception of ≠Gi, in large volumes. Together, these studies suggest that MSA populations in the region were highly mobile and repeatedly made costly choices (in terms of energy expenditure) with regard to both raw material source selection and items to be transported.

This study applies the combined use of silcrete provenancing and *chaîne opératoire* analysis to five newly excavated MSA sites in Ntswetwe Pan, part of the Makgadikgadi Pans complex in north-central Botswana (Fig. 1). Previous geochemical provenancing research in Botswana has focussed on repeatedly occupied (or visited) sites such as rock shelters and caves. In this study, we explore patterns of raw material procurement exclusively at open-

air sites. Such sites are normally associated with more transient use and might be expected to reveal differences in human behavioural patterns and the acquisition of raw materials encountered within a foraging range (e.g. Dietl et al., 2005; Will et al., 2013; Oestmo et al., 2014; Clark, 2017; Karlin and Julien, 2019; Shaw et al., 2019). Silcrete is more widely available within the Makgadikgadi Pans compared to previously investigated regions of northwest Botswana, making it possible to compare lithic raw material procurement patterns in different resource contexts. The Makgadikgadi Pans also offer a much more complex sedimentary and geochemical environment for silcrete formation than the mainly river and valley sites examined by Nash et al. (2013, 2016). This has required methodological innovations, including a move away from a provenancing approach that relies on statistical inference to match artefacts to particular silcrete sources to one that emphasises the geochemical and petrographic integrity of individual silcrete samples and outcrops.

The paper first summarises the geology, geomorphology and distribution of silcrete within the Makgadikgadi Pans. The characteristics of the five archaeological sites are then described. Factors influencing the chemistry of silcrete within Ntswetwe Pan are explored through an analysis of unconsolidated sediments underlying the largest of the archaeological sites. These results are used to underpin a comparison of the geochemistry of silcrete artefacts from Ntswetwe Pan against potential raw material sources from across the Makgadikgadi basin and adjacent areas of northwest Botswana. From this, raw material procurement patterns are identified, and the implications for understanding early human mobility in the Middle Kalahari discussed.

2. Background to the Makgadikgadi Pans

2.1. Geology and geomorphology of the Makgadikgadi Pans

The Makgadikgadi Pans complex (Fig. 1a) forms the lowest point of an endorheic drainage system that extends into Angola, Namibia and Zimbabwe (Baillieu, 1979; Cooke, 1980; Cooke and Verstappen, 1984; Burrough, 2022; Mendelsohn, 2022). Today, the Makgadikgadi has a precipitation to evapotranspiration ratio of 1:3 (Bhalotra, 1987). The pans are, however, subject to flooding during the austral summer rainy season (October–April), fed by direct rainfall and inflows from ephemeral rivers including the Nunga, Lememba, Nata, Semowane, Mosetse, Lepashe and Mosupe (Fig. 1b). Following years of heavy rainfall over tropical Angola, water may also enter the Makgadikgadi Pans via the Boteti River, the main connection to the Okavango Delta and Okavango drainage system (Wilson and Dincer, 1976; Cooke and Verstappen, 1984; Helgren, 1984; McCarthy and Ellery, 1998; Milzow et al., 2009; Burrough, 2022). As the lowest lying area of central Botswana, the pans are also the focus of regional groundwater flow (de Vries et al., 2000; Stadler et al., 2010; Lekula et al., 2018), with fault systems acting as conduits for recharge and enhanced groundwater movement (de Vries et al., 2000).

The Makgadikgadi Pans are situated within a complex tectonic deformation zone (Carney et al., 1994; Pastier et al., 2017). The underlying geology comprises variable thicknesses of Kalahari Group sediments that cover rocks of the Karoo Supergroup and Archaean basement (Haddon and McCarthy, 2005). The Karoo sequence includes Eccia, Beaufort and Lebung Group sediments overlain, in the southernmost Makgadikgadi, by Stormberg Group flood basalts (Smith, 1984; Franchi et al., 2021). Escarpments of Karoo basalt and sandstone delimit the southern margins of the basin. High-grade metamorphic and igneous rocks of the Archaean Zimbabwe Craton outcrop to the east within the Nata, Semowane,

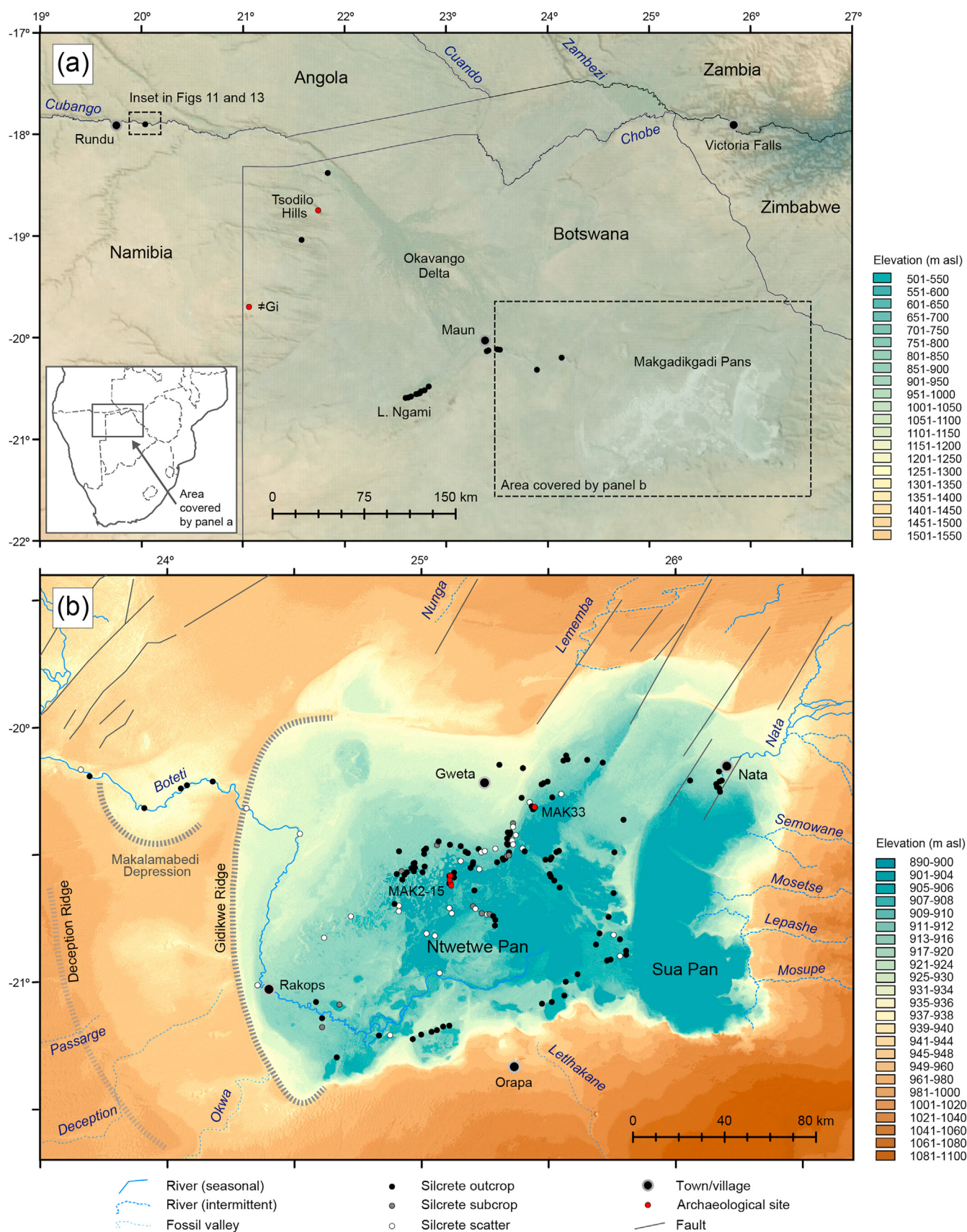


Fig. 1. Geomorphology of the Makgadikgadi Pans complex, including locations of archaeological sites and silcrete sampling sites from (a) 2011 and (b) 2016–2017 field seasons. The Middle Stone Age archaeological sites White Paintings Shelter, Rhino Cave and Corner Cave are all located within the Tsodilo Hills (panel a).

Mosetse, Lepashe and Mosupe catchments (Mallick et al., 1981; Carney et al., 1994; Key and Ayres, 2000; Kampunzu et al., 2003).

Debates around the hydrological history of the Makgadikgadi basin are summarised in Burrough (2022). Some authors (e.g. McFarlane et al., 2005; Moore et al., 2012) propose that the basin remained largely inactive during the Pleistocene. Others, based on a growing body of geochronological data, suggest that high lake stands (or 'megalakes') recurred periodically over the late Quaternary (e.g. Cooke and Verstappen, 1984; Shaw et al., 1997; Burrough et al., 2009; Schmidt et al., 2017). At its maximum, the late Quaternary megalake system is suggested to have covered at least 66,000 km² of the Middle Kalahari (White and Eckardt, 2006), with this maximum level reached on multiple occasions in the last 200 kyrs (Burrough et al., 2009). Megalake phases were likely fed by backflooding from the Zambezi (via the Chobe) and inputs from the Boteti, easterly rivers and the now-fossil Okwa, Mmone/Quoxo, Deception and Letlhakane systems (e.g. Shaw et al., 1992; Nash and Eckardt, 2016; Nash, 2022a), plus groundwater sources.

2.2. Silcrete in the Makgadikgadi Pans

Although its distribution has not been mapped, the Makgadikgadi basin likely contains the greatest surface exposure of silcrete in the Kalahari. The main areas of occurrence include the floors and margins of pans and ephemeral rivers, and within cemented palaeolake shorelines (e.g. Mallick et al., 1981; Summerfield, 1982; Shaw et al., 1990; Nash and Shaw, 1998; Shaw and Nash, 1998; Ringrose et al., 2005, 2009, 2014). In Ntwetwe Pan, silcrete is commonly encountered as a gravel-to cobble-sized surface lag on the pan floor (here termed a silcrete 'scatter'), suggestive of the breakup of former buried groundwater silcrete layers (Nash, 2022b). Silcrete scatters vary in scale from 10s to many 100s of square metres, with the most extensive spreads found along the

eastern and south-central margins of Ntwetwe. Where surface outcrops occur, they are usually localised and vary from decimetre scale mounds (e.g. foreground of Fig. 2a) to layers up to 2 m thick (in the bed of the Boteti; Fig. 3a). Many silcretes occur in association with calcrete and silcrete-calcrete intergrade duricrusts, reflecting the dynamic chemical environment of the pan (Nash and Shaw, 1998; Ringrose et al., 2009; Nash, 2022b).

Silcretes in the Makgadikgadi exhibit a variety of morphologies. In part, this depends upon whether the silcrete formed as a primary precipitate within fluvial or lacustrine sediments or developed via the replacement of a pre-existing calcrete (Nash and Shaw, 1998; Nash et al., 2004). Primary silcretes, such as those exposed along the Boteti and Nata rivers and across large areas of the pans, are typically nodular, sheet-like or massive in appearance (Fig. 2). Those that formed by replacement of calcrete have more irregular morphologies (Ringrose et al., 2009). The range of morphologies encountered across Ntwetwe Pan (Fig. 2) – including unusual tube-like silcretes likely formed via the silicification of root structures – is illustrative of the wider variability.

The colour of individual silcrete outcrops and scatters varies from pale to dark green in the case of glauconitic silcretes at the northern and southern margins of the Makgadikgadi (see Boocock and van Straten, 1962; Summerfield, 1982; Webb and Nash, 2020), to white, grey, cream, buff, brown, reddish-brown and black elsewhere. These colours are rarely uniform, with many silcretes including darker or lighter flecks, veins and inclusions or – in the case of silcretes along the Boteti River – 'whorl'-like patterns of iron hydroxide staining within the silica cement (Summerfield, 1982). Exceptions include the outcrops and extensive scatters of dark grey to black silcrete found in pan-marginal areas of eastern and south-central Ntwetwe, which are much more uniform in colour.

The majority of outcrops associated with fluvial inflows are likely to have formed as drainage-line silcretes (Nash and Ulliyott,

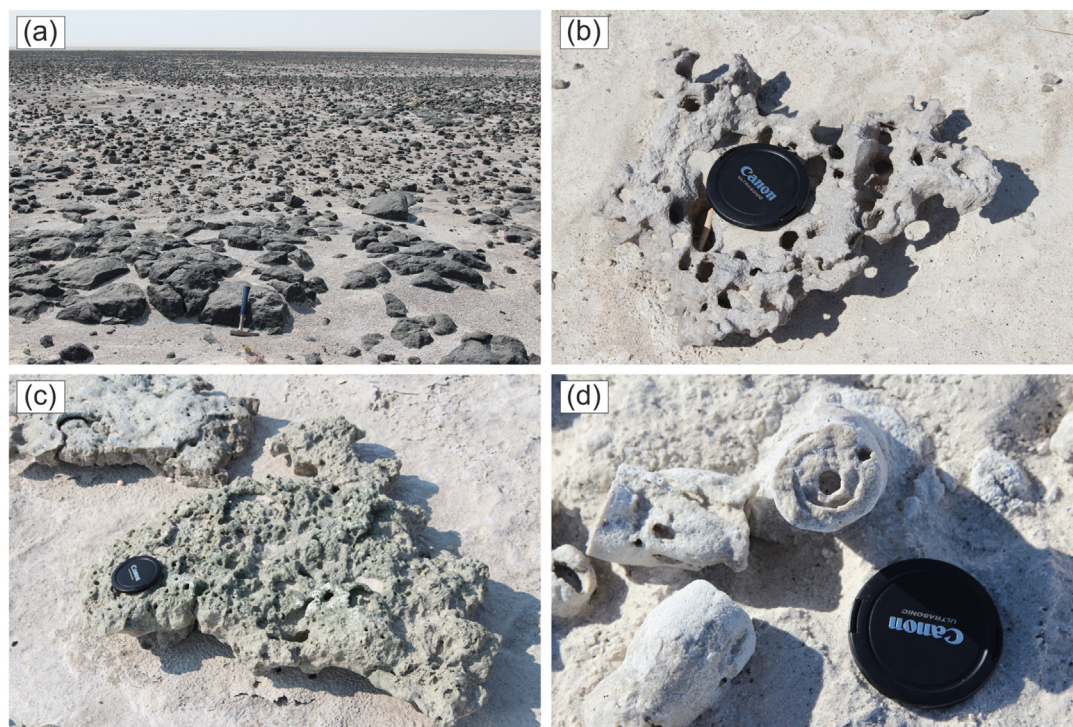


Fig. 2. Variations in silcrete morphology across Ntwetwe Pan. (a) Low outcrops of black silcrete surrounded by an extensive scatter of black silcrete fragments; (b) thin 'honeycomb' silcrete sheet formed by the merger of individual silcrete nodules close to a former water table; (c) decimetre-scale sheet-like silcrete with vertical hollows, likely formed by the progressive silicification of a 'honeycomb' silcrete; (d) rare silicified tube-like structures suggestive of former roots. Locations of images: (a) south-central Ntwetwe Pan (b–d) north-central Ntwetwe Pan.

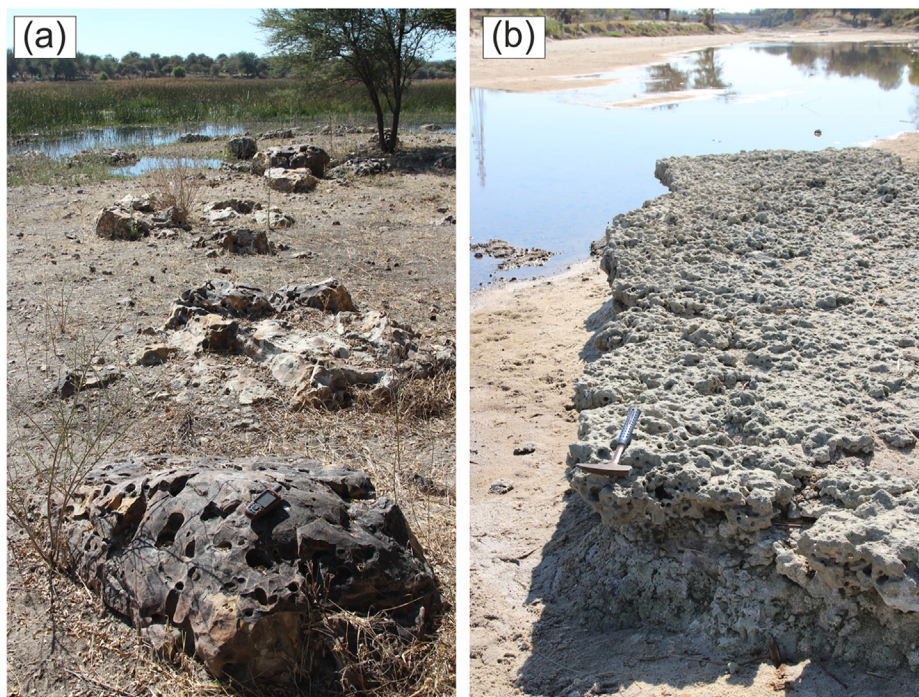


Fig. 3. Silcrete outcrops within fluvial inflows into the Makgadikgadi Basin. (a) Massive drainage-line silcrete near Samedupi Drift on the Boteti River; (b) Nodular drainage-line silcrete in the bed of the Nata River downstream of Nata village.

2007), i.e. through the accumulation of a clastic silica host sediment transported by floodwaters alongside precipitation of amorphous silica from shallow groundwater (Shaw and Nash, 1998). Silcretes in pan-floor settings likely formed close to a former water table, with silica precipitation driven by changes in salinity and pH (Thiry, 1999). Monitoring of the hydrochemistry of Sua Pan over two wet seasons has shown that the pH of lake waters ranged between pH 8.6 and 10, with the lowest pH following influxes of rain- or flood-water (Eckardt et al., 2008; McCulloch et al., 2008). Such dynamic environmental conditions facilitate both the mobilisation of silica (from quartz grains and biogenic silica sources as pH increases above pH 9) and its re-precipitation (as pH falls to below pH 9; see Nash and Ulliyott, 2007). The zone of maximum mixing of fresh and more saline lake waters is likely to occur around evaporitic depressions and immediately above the water table (Thiry, 1999). Silicification often occurs marginal to pans and may be linked to regression or to areas of near-surface perched groundwater (e.g. Summerfield, 1982; Bustillo and Bustillo, 1993; Armenteros et al., 1995; Alley, 1998; Bustillo and Bustillo, 2000; Ringrose et al., 2005). This phenomenon is well-illustrated in the Makgadikgadi, where silcrete lenses in lake-marginal duricrust sequences appear to have formed in association with former water tables (Summerfield, 1982). Biological fixing of silica has also been documented, with sheet-like silcretes in Sua Pan developed as a result of the desiccation of formerly floating colonies of the silica-fixing cyanobacteria *Chloriflexus* (Shaw et al., 1990).

3. Characteristics of archaeological sites

In this study, geochemical data are analysed to match silcrete artefacts from five newly-excavated open-air MSA sites on the floor of Ntwetwe Pan to their potential raw material sources. Site and sample numbering conventions are provided in the Supplementary Data. Four sites – MAK2, MAK14K, MAK14O and MAK15 – are situated in the central pan, while the fifth, MAK33, is in

northeastern Ntwetwe (Fig. 1b). The sites fall into three categories based on the size of the excavated area and lithic assemblage – small (<25 m²; MAK2, MAK15), medium (50–100 m²; MAK14K, MAK14O) and large (>400 m²; MAK33) – and are described in this order. The detailed characteristics of each site, and the excavation strategy and analytical approach used, are documented in Staurset et al. (2022a).

All five sites exhibited clearly delineated lithic spreads that included a varying number of tool production stages, with limited indications of post-depositional disturbance. Sites were excavated using a *décapage* approach (see Enloe, 2004; Olive, 2005; Julien and Karlin, 2015). An excavation grid covering all visible artefact concentrations was established at each site, and extended to document the location of outliers. The overburden at all sites comprised a scant loose deposit (see Fig. 4 a,b); removal of this deposit established that artefact assemblages were lying directly on the pan surface. Testing below 5 cm depth confirmed that little archaeological material was located below the surface. Some grid squares at each site, both below artefact concentrations and at site margins, were dug to depths of up to 1 m for sampling for dating and palaeoenvironmental analysis (e.g. Fig. 4d). Only one of these deeper pits (at site MAK33) uncovered a potential MSA flake. Grid squares were photographed to record the spatial position of artefacts, after which artefacts were removed, numbered and curated.

Artefacts at all five sites were in very fresh to mint condition. In contrast to other Kalahari MSA sites, the only raw material employed in tool production was silcrete. All sites were characterised by the production of heavily retouched unifacial and bifacial points (e.g. Fig. 4c), produced either on natural blanks or on flakes originating in Levallois, Kombewa or discoidal reduction strategies; tool types other than points were rare (see Coulson et al., 2022; Staurset et al., 2022a).

Sites **MAK2** (excavated area 24 m²; 38 artefacts) and **MAK15** (22 m²; 55 artefacts) are located on the pan floor, adjacent to small, morphologically-indistinct, vegetated dunes (Richards et al., 2021).

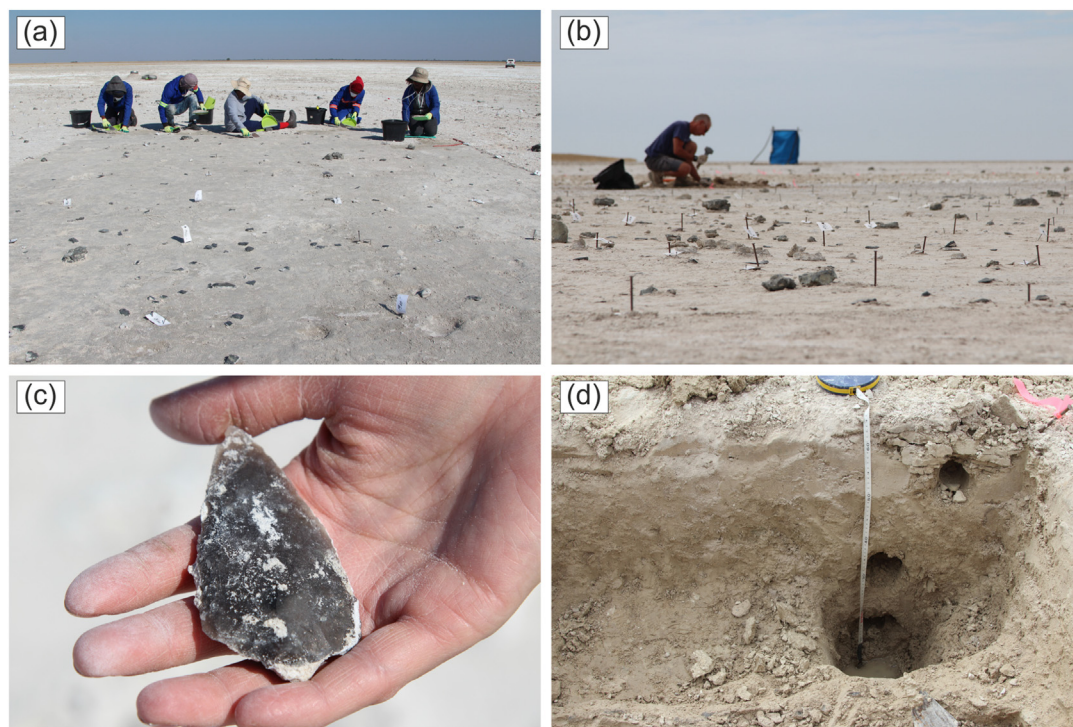


Fig. 4. Overview of archaeological site MAK33 in Ntwetwe Pan. (a, b) General views of site, showing the nature of the surface sediment and diversity of silcrete artefacts present. (c) Example of a diagnostic Middle Stone Age point manufactured from black silcrete. (d) Oblique view of pit dug west of main excavation area within the site (environmental sampling site MAK/17/8 in Burrough et al., 2022); sample locations for OSL dates MAK/17/8/1 (13 cm depth), MAK/17/8/2 (35 cm) and MAK/17/8/3 (50 cm) are visible to the right of the image.

These features are relatively young; optically-stimulated luminescence (OSL) dating suggests that the dune adjacent to MAK15 was formed during a phase of aeolian accumulation as recently as 80 ± 10 years ago (see Burrough et al., 2022, for details). Knapping efforts are restricted to later stages of the *chaîne opératoire* of point production and, given the small assemblage sizes, probably represent brief re-tooling episodes. Local production sequences at each site are disjointed, as confirmed by the small number of refits (Staurset et al., 2022a).

Sites **MAK14K** (excavated area 42 m²; 88 artefacts) and **MAK14O** (100 m²; 555 artefacts) form part of an unusually rich zone of c. 250 × 600 m that includes 15 archaeological sites and scatters, as well as numerous loose finds (Staurset et al., 2022a). MAK14K was situated next to a small lake-bed dune (formed around the same time as the dune at MAK15; Burrough et al., 2022), whilst MAK14O was on open pan floor. The vast majority of the assemblage at MAK14K comprises a grey-black silcrete. Retouched pieces cluster in one area of the site (Staurset et al., 2022b). Cores and core fragments only feature outside this cluster, potentially reflecting the discard of exhausted examples, with partially worked cores removed from the site along with finished tools. More stages of the *chaîne opératoire* are present at MAK14K compared to the smaller sites. However, there are no indications of core cleaning or evidence of full reduction sequences. Once again, the number of refits is limited, likely due to disjointed local production sequences. The assemblage at MAK14O is dominated by a distinct black silcrete worked with a consistent pattern of production techniques. This material displays all stages of the *chaîne opératoire*, including the initial testing of a raw material block, core cleaning, blank production and discard of exhausted cores. Additional smaller silcrete raw material groups represent either finishing stages of point manufacture or abandonment of rejected examples.

At **MAK33**, the largest visible concentrations of artefacts fell within an excavated area of 430 m² (Fig. 4b); a >4000 m² zone

beyond this area was surface collected and all finds incorporated within an extended grid. In total, 3426 artefacts were recovered. The vast majority of the assemblage was recovered from the surface level; excavation to 5–10 cm, where possible, only increased the assemblage size by <0.5%. Three areas comprising denser artefact spreads can be identified, designated as MAK33 West, North and South (see Staurset et al., 2022b, for details). In the West, several knapping concentrations, comprising debris, cores and tools in various stages of manufacture, are present. Analogous lithic material was found in the North and South, but here concentrations are more diffuse. A substantial number of refits were made (c. 21% of the assemblage). Several knapped blocks were reconstructed, allowing their original size to be estimated. Refitting also revealed surprisingly complete production sequences. Plotting these sequences indicated where cores were originally worked and showed that some artefacts had been moved from where they were originally struck, linking areas West, North and South, as well as some additional zones (Staurset et al., 2022a).

OSL age estimates were generated for four of the five archaeological sites. For three sites, it was only possible to infer a maximum age based on dating the sediment immediately below the surface artefact layer: 106 ± 3 ka for site MAK14O; 70 ± 12 ka for MAK15 and 69 ± 7 ka for MAK33 (see Burrough et al., 2022, for full details). At MAK14K, minimum and maximum age estimates for site formation could be determined. As noted above, this site was immediately adjacent to a recent lake-bed dune. An investigative trench dug into this dune and the underlying lake-bed sediments revealed a silcrete flake between two chronostratigraphically distinct layers of lake-bed sediment. The artefact lay on top of muddy lake-bed sands deposited at 84 ± 10 ka; this sand layer extended out into the MAK14K site where it was also dated to between 85 ± 10 and 92 ± 4 ka. Silty sands overlying the artefact were dated to between 57 and 59 ± 8 ka, constraining site use to a window of c. 20 kyr.

Analyses by Burrough et al. (2022) tentatively suggest that the

four dated archaeological sites both post-date (overlie) and pre-date (underlie) lake sediments deposited during a lake high-stand that occupied the Makgadikgadi basin sometime between 72 and 57 ka. This high-stand is documented within shoreline records, which infer that lake levels between 66 and 60 ka were 37–39 m above the present lake floor (see Burrough et al., 2009; de Cort et al., 2021). Burrough et al. (2022) argue that the archaeological sites are visible on the floor of Ntswetwe Pan today due to the removal by deflation of any sediments from subsequent high-stands deposited at these locations. This mechanism would also explain the fresh condition of the exposed silcrete artefacts at all sites. In other parts of the basin, wetter conditions limit aeolian erosion, leading to lesser deflation and the longer preservation of sediments deposited during wet phases.

4. Materials and methods

Two main phases of sampling and analysis were used in this study. First, silcrete outcrops and areas of silcrete scatter were sampled from across the Makgadikgadi basin (referred to collectively as 'outcrop samples'). Second, geochemical data were obtained from selected outcrop samples and archaeological artefacts. In parallel with these investigations, geochemical analyses of unconsolidated pan floor sediments from a pit dug within archaeological site MAK33 (Fig. 4d) were undertaken to assess the potential controls upon silcrete chemistry in Ntswetwe Pan. The main sampling and instrumental analytical methods are described here. For the approach used to compare the geochemistry of outcrop samples and artefacts, see section 6.

4.1. Sampling of silcretes and pan-floor sediments

Central to the success of any geochemical fingerprinting approach is the chemical characterisation of potential raw material sites. Our target for fieldwork was to sample as many silcrete outcrops and scatters within and around Ntswetwe Pan as possible. This involved extensive vehicle-based reconnaissance during two field seasons in 2016 and 2017. The identification and sampling of outcrops was straightforward in open, unvegetated areas of Ntswetwe Pan, where the typically darker silcrete stood out against the white pan floor sediments. The only area of open pan floor that could not be reconnoitred was the southeastern sector, where flooding in early 2017 had rendered the sediment surface unsafe for driving and therefore inaccessible; the unvegetated pan edges in this area were, however explored. Reconnaissance around the vegetated margins of Ntswetwe Pan, including along palaeolake shorelines in northeast and north-central areas of the pan, was restricted to access along formal and informal tracks. Access into areas of Ntswetwe with large numbers of vegetated lake-bed dunes, including in the extreme west and east of the pan, was challenging, but good geographical coverage was achieved.

Samples were collected at 96 sites in and around Ntswetwe Pan in 2016 and at a further 91 sites in 2017. All sampling sites were in primary context – the extremely low gradient of the pan environment precludes the erosion and transport of silcrete cobbles and, hence, the development of secondary sources at distance from their origin. Sites were foot-surveyed prior to sampling, with four representative c.150 g samples collected at the majority of locations; three were used for geochemical analysis with the fourth retained as a reference. For sites where silcrete outcropped at the surface, samples were collected at regular vertical intervals down the outcrop. For silcrete scatters, the samples were selected randomly. A GPS reading was taken at each site.

Samples of unconsolidated pan-floor sediment were collected at 5 cm vertical intervals down the face of a 65 cm deep pit dug west

of the main excavation area within archaeological site MAK33 (Fig. 4d). Sediment within the pit comprised weakly silica-cemented sands, silt and clay throughout, with laminations showing on drying (Burrough et al., 2022).

4.2. Selection of silcrete artefacts from archaeological sites

To compare artefacts from the five MSA sites (section 3) to their potential sources, manufacturing waste flakes from each site were sampled for geochemical analysis. Following excavation, cleaning and labelling, the lithic assemblages were analysed and classified as described in Staurset et al. (2022a,b); a brief summary is given here. As part of early stage *chaîne opératoire* analysis, the assemblage from each site was separated into silcrete raw material groups based on hand specimen characteristics (i.e. grain size, fracture pattern, degree of cementation, level of translucence, type of cortex, the occurrence of rinds, overall colour and the presence of specks or patches of varying colour; see Staurset et al., 2022b). Colour was found to be a misleading characteristic, as a number of refitted blocks exhibit within-block colour changes. The resulting raw material groups formed the starting point for identifying artefacts that likely originated from the same block, and were further tested and refined through refitting. This procedure is an extended version of that employed in earlier silcrete provenancing investigations in northwest Botswana (Nash et al., 2013, 2016). However, individual blocks of silcrete from the Ntswetwe Pan sites display more internal variability and are less easy to separate into distinct raw material groups compared to these studies. Sample manufacturing waste flakes were selected subsequently to represent the variability of material present at each site, with more samples included from raw material groups with larger numbers of artefacts or greater variability; see Table S1 in the Supplementary Data for full details.

4.3. Geochemical analysis

Of the 187 outcrops and scatters where samples were collected, 110 sites within the vicinity of Ntswetwe Pan were identified for geochemical analysis. Sites that were omitted fell into three categories: (i) sites along the Boteti River that overlapped with the sampling framework of Nash et al. (2013) and where chemical data were therefore already available; (ii) densely sampled outcrops and scatters of black silcrete along the pan margin in south-central and eastern Ntswetwe (where samples from alternating sites only were analysed); and (iii) sites along the southernmost margin of Makgadikgadi between Rakops and Orapa and along the Nata River north of Sua Pan. All 46 selected artefacts were analysed.

Details of the techniques used to prepare and analyse silcrete outcrop samples, artefacts and unconsolidated pan-floor sediments are given in the Supplementary Data. Of the 324 outcrop samples analysed, 235 comprised >80 wt % SiO₂ and can be classified as silcretes. The remaining 89 outcrop samples contained SiO₂ in the range c.55–80 wt % and would be classified as the intergrade duricrustal-silcrete (see Nash and Shaw, 1998); data from these samples were not used in subsequent analyses. The silcrete dataset generated for this study was expanded by the addition of equivalent data for 86 silcrete samples containing >80 wt % SiO₂ collected at 28 sites in northwest Botswana and northern Namibia in 2011. These samples were processed in the same laboratory as the present study, using the same protocols for sample preparation and analysis; data are available in the supplementary materials of Nash et al. (2013).

5. Chemical variability within unconsolidated pan-floor sediments in Ntwetwe Pan

Fig. 5 shows down-profile variations in immobile trace element ratios within the unconsolidated pan-floor sediments adjacent to the western edge of the MAK33 excavation. Values in panels (a) and (b) show coherent variability with depth. Changes in these element ratios beyond instrumental uncertainty (as indicated by the x-axis error bars) occur below 25, 40, 45 and 60 cm depth and can be used to distinguish five layers with distinct geochemical signatures (labelled 1–5). Layers 2 and 4 are similar in terms of the element ratios in panels (a) and (b) but can be distinguished further as a result of differences in Ti/Zr (Fig. 5d). Similarly, layers 3 and 5 differ mainly in their Nb/Zr and Ti/Zr values (Fig. 5c and d).

The distinct down-profile geochemical signature differences within the pan-floor sediments most likely reflect the proportional sediment input into Ntwetwe Pan from fluvial systems with different catchment geologies. It is also feasible that the chemical variations are the result of sediment input via inflows of different magnitudes from the same fluvial system(s). These scenarios are illustrated in Fig. 6. The co-variance of Nb/Zr and Ti/Zr may, for example, simply reflect fluctuations in the quantity of the Nb- and Ti-bearing mineral rutile transported into the pan, coupled with differential deposition under variable flow energy states. Site MAK33 is relatively close to the margin of the modern pan, and may have been affected by water level and inflow changes to a greater extent than locations nearer the depocentre of the Makgadikgadi basin.

Trace element data plot closely together on Th–Sc–Zr and La–Th–Sc tectonic discrimination diagrams, and show that the Ntwetwe pan-floor samples are similar in composition to sediments deposited on continental margins today (inset panels in Fig. 7a and b). Substituting the generic tectonic fields of Bhatia and Crook (1986) for compositional fields of potential catchment geologies allows further discrimination. On the Th–Sc–Zr diagram (main panel, Fig. 7a), the Ntwetwe pan-floor samples sit within the compositional fields for Congo Craton granitic lithologies and Karoo sediments. On the La–Th–Sc diagram (main panel, Fig. 7b), the samples sit entirely within the fields for Zimbabwe Craton and Congo Craton

granitic lithologies, and partly overlap with the field for Karoo sediments. The distribution of data most strongly suggests that the Ntwetwe pan-floor sediments were derived from granitic cratonic rocks most similar to those found in the Congo Craton (the only source that overlaps entirely with the Ntwetwe samples). This conclusion is consistent with the original mineral detritus within the pan-floor sediments being derived mainly from the Okavango catchment – which has headwaters in the southwest Congo Craton (Fig. 7c) – and transported into the Makgadikgadi basin via the Okavango Delta and Boteti River. The lack of Sc within the sediments indicates they contain very little mafic material, precluding any significant input from catchments to the south of the Makgadikgadi underlain by Karoo basalt.

OSL ages from three samples from the MAK33 sampling pit were within errors for the whole profile and ranged from 94.2 ± 7.2 to 80.5 ± 6 ka (Burroughs et al., 2022). It is not possible to tell if each chemically-coherent layer in Fig. 5 reflects a separate flood event entering Ntwetwe around this time or is an amalgamation of multiple flood events fed by the same fluvial catchment(s). Abrupt changes in the chemical profile may represent erosive boundaries generated by flood events but could also reflect where sediment has been removed via aeolian deflation. Gradual changes within layers may represent longer term shifts in the make-up of detrital minerals being liberated from individual catchments, or possibly fining-upwards sequences.

Regardless of the drivers of the chemical variability seen in Fig. 5, these results have important implications for understanding the generation of the geochemical signatures of silcretes within the Makgadikgadi Pans complex. Meta-analysis of geochemical data for Kalahari silcretes and their host sediments has shown that the immobile trace element composition of the parent sands is retained during silicification and any subsequent weathering (Webb and Nash, 2020). The silicification of a sediment sequence such as that shown in Fig. 5 to form a silcrete profile would therefore be expected to preserve the multiple geochemical signatures evident in the sequence. If, as illustrated in Fig. 6, a silcrete profile were then eroded to form a silcrete scatter, the scatter would retain an equally complex geochemical picture. Following this argument, individual silcrete outcrops or scatters within the Makgadikgadi Pans could

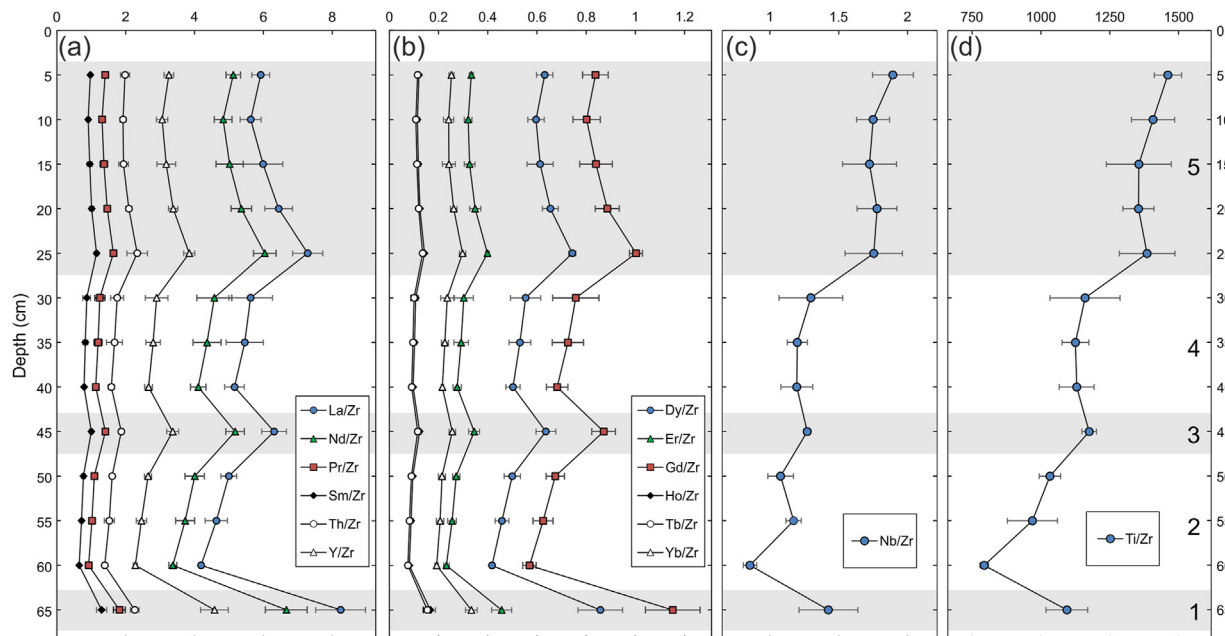


Fig. 5. (a–d) Variations in immobile trace element ratios with depth within unconsolidated pan floor sediments from archaeological site MAK33 in Ntwetwe Pan. Grey block shading is used to distinguish sediment layers with a coherent trace element signature. X-axis error bars reflect ± 3 standard deviations from the mean value for each element ratio.

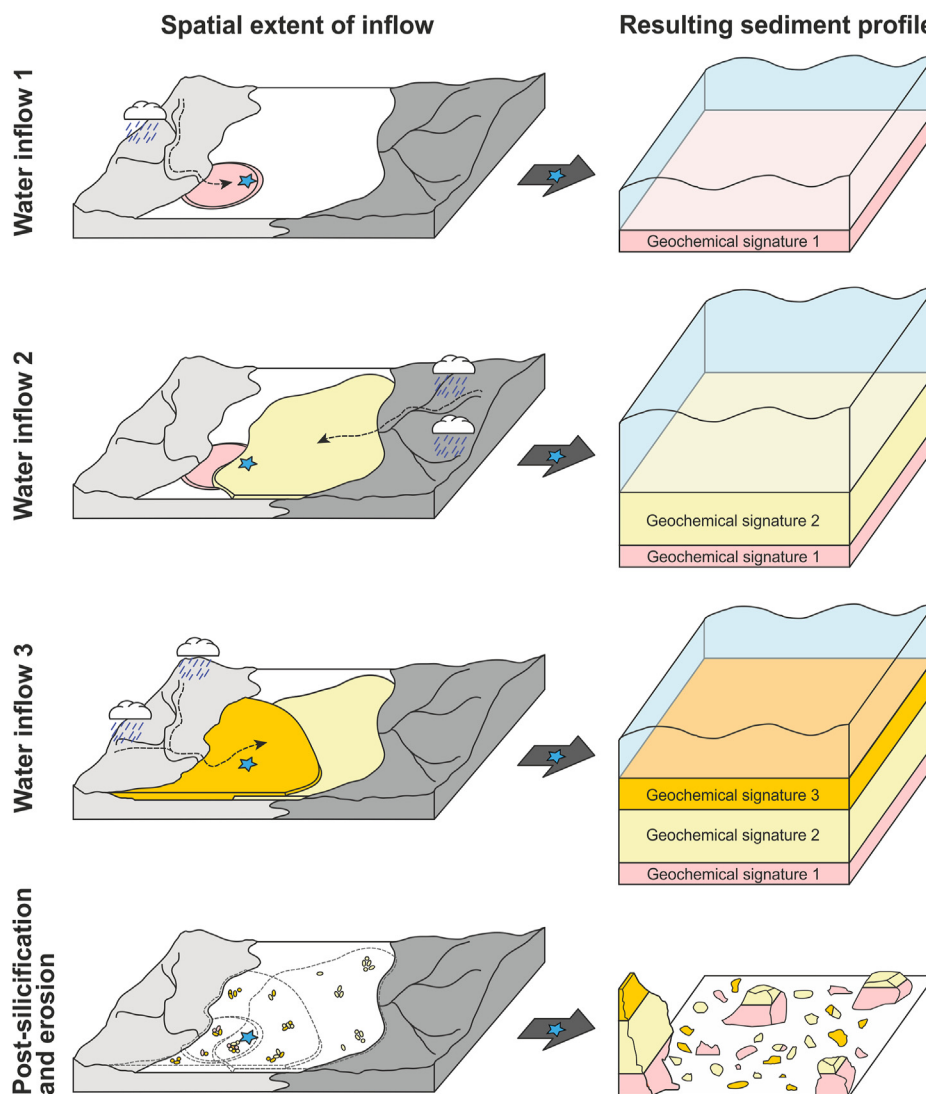


Fig. 6. Example of how water inflows from different catchment areas and of different event magnitudes could generate a basin-floor sediment profile with multiple immobile trace element signatures (top three panels). A silcrete scatter with multiple trace element signatures would be produced if this sediment sequence was silicified and then broken up by erosion (bottom panel).

exhibit multiple geochemical signatures. Further, if the water influx that deposited a particular sediment layer inundated a large area of the pans (as illustrated by inflow events 2 and 3 on Fig. 6), it is possible that the same geochemical signature could be present in silcretes in different locations. The significance of these findings for raw material provenancing are considered in the next section.

6. Spatial patterns of raw material procurement within Ntswetwe Pan

6.1. Approach used to compare silcrete artefact and outcrop properties

The approach used by Nash et al. (2013) to compare the chemistry of silcrete artefacts with silcrete outcrops relied upon linear discriminant analysis of geochemical data, with outcrops grouped according to geographical area. This statistics-based approach was effective in northwest Botswana where silcretes in four distinct geographic areas were shown to contain markedly different concentrations of trace elements. However, the recognition that a single silcrete outcrop or scatter in the Makgadikgadi Basin could

exhibit more than one distinct geochemical signature (section 5) renders this statistical approach inappropriate for this study. Instead, the comparison of artefact and outcrop chemistry followed the geochemical fingerprinting protocol introduced by Nash et al. (2020) in their analysis of silcretes at Stonehenge, UK. Under this approach, ICP-MS data were used to generate an “immobile trace element signature” for each silcrete artefact and outcrop sample – effectively a graphical plot of selected trace element data for each sample – that were then compared. The signatures were constructed using concentration data for Dy, Er, Gd, Hf, Ho, La, Nb, Nd, Pr, Sm, Tb, Th, Ti, Tm, Y, Yb and Zr only. These elements were selected on the basis that they are normally immobile in the near-surface weathering environments encountered in the Makgadikgadi, hence there should be no enrichment or depletion of elements over the time since the silcrete formed (see Middelburg et al., 1988; Pearce, 1996; Neck and Kim, 2001). Further, these elements were all measured with an instrumental precision of 1 ppm or better, and were recorded at or above detection limits in >90% of silcrete outcrop samples. Nash et al. (2020) used data for a further five trace elements (Ba, Ce, Rb, Sr, U) in the generation of their geochemical signatures. However, pH and redox fluctuations in the

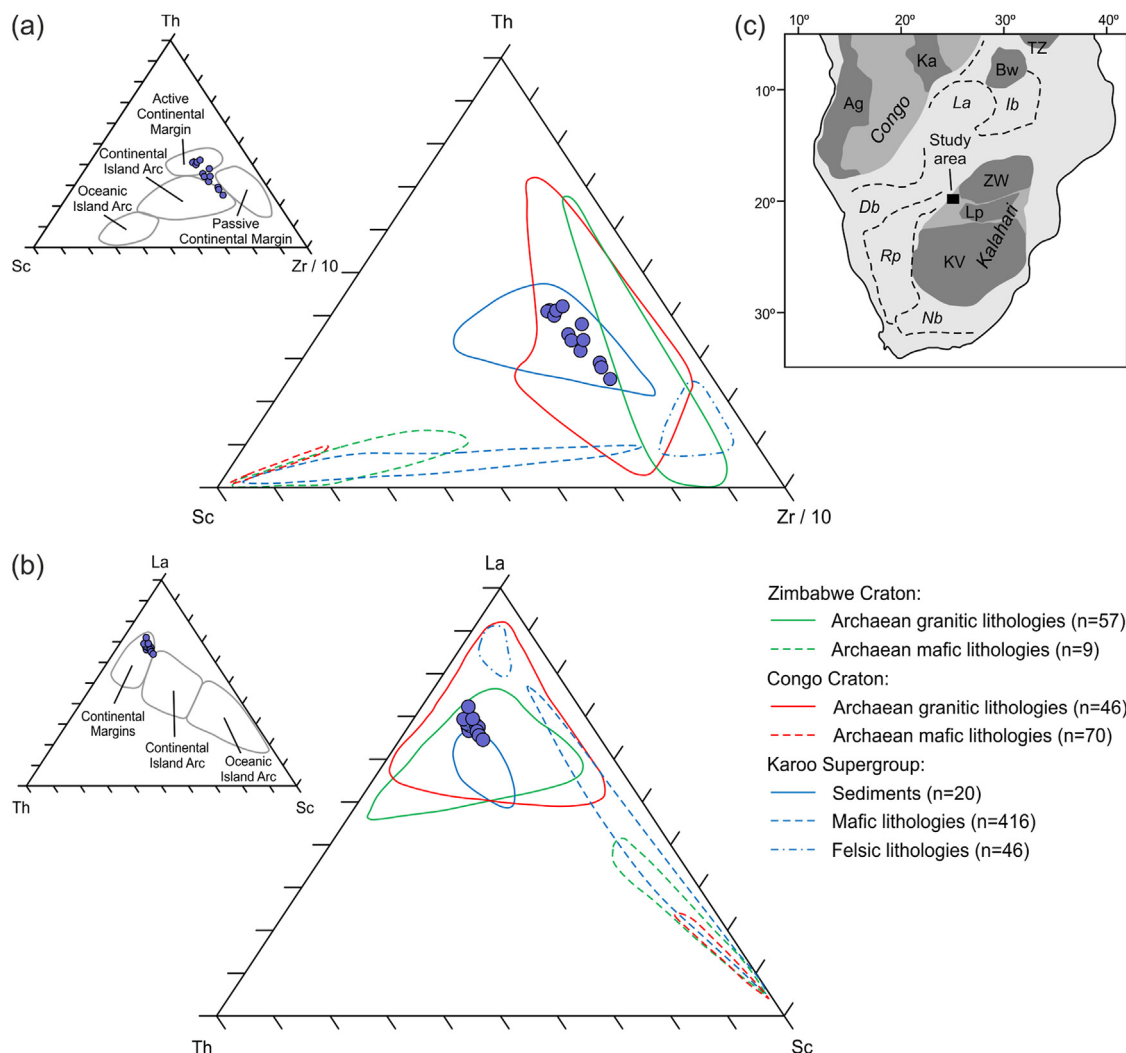


Fig. 7. (a) Th-Sc-Zr and (b) La-Th-Sc tectonic discrimination diagrams for unconsolidated pan-floor sediment samples from archaeological site MAK33 in Ntwetwe Pan. Main panels show data plotted against compositional fields for potential sediment sources, including Archaean-Proterozoic granitic and mafic lithologies from the Zimbabwe Craton (Bolhar et al., 2003; Sossi et al., 2016; Greaney et al., 2018; Wagner et al., 2021) and Congo Craton (Maier et al., 2015; Turnbull et al., 2021), and sedimentary, mafic and felsic lithologies from the Phanerozoic Karoo Supergroup (Jourdan et al., 2007; Miller and Harris, 2007; Galerne et al., 2008; Neumann et al., 2011; Kamenetsky et al., 2017; Turunen et al., 2019; de Wit et al., 2020); n indicates the number of analyses used to delimit each compositional field. Inset panels show data plotted against tectonic domains defined by Bhatia and Crook (1986). (c) Congo Craton, Kalahari Craton and other primary features of the pre-Karoo geology of southern Africa (after Celli et al., 2020). Archaean shield areas are plotted in dark grey: Ag Angola, Bw Bangweulu Block, Ka Kasai, KV Kaapvaal, Lp Limpopo Block, TZ Tanzania, ZB Zimbabwe. Mobile belts are demarcated by black dashed lines: Db Damara, Ib Irumide, La Lufilian Arc, Nb Namaqua, Rp Rehoboth Province.

Makgadikgadi Pans are of sufficient magnitude that they could promote mobility of these elements (see Eckardt et al., 2008), so they were omitted in this study.

For each silcrete sample or artefact, the concentrations (ppm) of Dy, Er, Gd, Hf, Ho, La, Nb, Nd, Pr, Sm, Tb, Th, Ti, Tm, Y and Yb were normalised by dividing by the Zr concentration (ppm) of that sample/artefact, producing 16 unitless trace element ratios per sample. Normalisation was used to overcome the effects of variable silicification upon trace element concentrations. During silcrete formation, the introduction of silica into the host sediment increases the SiO₂ content of the whole rock (Summerfield, 1982, 1983), and, as a result, decreases the relative concentration of every other element that might have been present within the original sedimentary detritus. Depending upon the extent of silicification (which can vary at the outcrop or even hand-specimen scale; Nash et al., 2004), this effect will be variable, meaning that two silcrete samples developed from the same homogenous host sediment could have different overall trace element abundances. Variable

silicification will not, however, change the trace element ratios within the sediment, because all trace elements will be doped equally by the introduced silica. Zr was selected as the denominator for normalisation as it was detected in all samples and, as a highly immobile element, is extremely unlikely to have been remobilised in the pan environment.

Y-axis error bars were calculated using quality control data for Certified Reference Materials (CRMs) obtained in the same analytical batch as the silcrete samples/artefacts (CRM data are available at <https://doi.org/10.17033/DATA.00000286>). To calculate the error bars associated with each set of analyses, the percentage difference in trace element concentration between the published and quality control values was calculated for each CRM to give a measure of analytical uncertainty (%) for each element. The analytical uncertainty for each element and the analytical uncertainty for Zr were then summed to give the analytical uncertainty (%) for each Zr-normalised trace element ratio. The standard deviation (σ) in analytical uncertainty was calculated from the resulting

data. To define the maximum (minimum) y-axis error bars for each silcrete sample and artefact, three times this standard deviation value was added to (subtracted from) each Zr-normalised trace element ratio. The resulting error bars give the maximum and minimum range for each Zr-normalised trace element ratio within the analytical limits of the ICP-MS instrument.

The immobile trace element ratio plots from each sampling site were scrutinised to assess whether – following the results reported in section 5 – the silcrete samples at each site had developed within layers of lacustrine sediment with similar or variable geochemical signatures. The process of cross-checking is shown in Fig. 8. For two samples to have formed within sediment with a common signature, the ranges for each of the 16 immobile trace element ratios would be expected to overlap within the limits of analytical error. This was found to be the case at 20 sampling sites. In the example shown (site BOT16/81), the silcrete samples can be seen to exhibit two distinct geochemical signatures – one comprising the “chemical continuum” formed by samples BOT16/81/1 and BOT16/81/2 and one from a single sample (BOT16/81/3) with distinctly higher values for Nb/Zr and Ti/Zr.

A similar process (see Nash et al., 2020) was used to determine

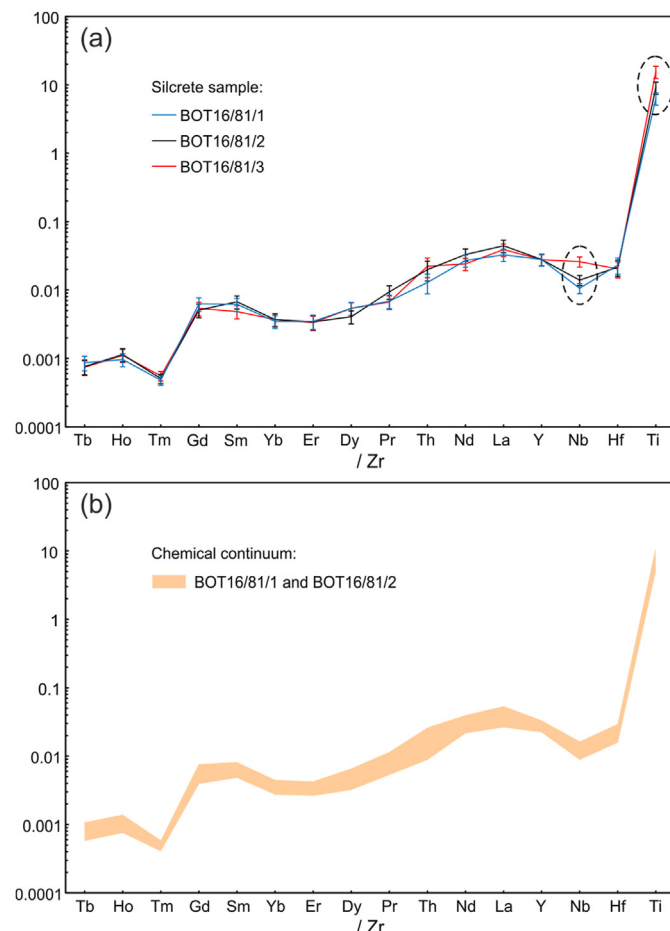


Fig. 8. Defining a chemical continuum at a silcrete sampling site, using an example from site BOT16/81. (a) The geochemical signatures for samples BOT16/81/1 and BOT16/81/2 show 100% overlap (within the limits of analytical error) for all immobile trace element ratios and form a chemical continuum. Sample BOT16/81/3 does not provide total overlap with either BOT16/81/1 or BOT16/81/2, indicating a discrete geochemical signature. The major differences between the samples are for Nb/Zr and Ti/Zr (circled), likely driven by BOT16/81/3 containing higher amounts of Nb- and Ti-bearing rutile. (b) The maximum (minimum) y-axis error bars for samples BOT16/81/1 and BOT16/81/2 are used to define the upper (lower) range of the chemical continuum.

the most likely raw material source of each artefact. The geochemical signature for each artefact was compared against the signatures for the 321 individual silcrete outcrop samples and 20 continua. A permissible match between an artefact and a silcrete sample (or continuum) was identified only where the range of all 16 immobile trace element ratios for the artefact and silcrete sample (or continuum) overlapped. Examples of permissible matches are shown in Fig. 9. This geochemical method is, we argue, more robust than probability-based statistical approaches to raw

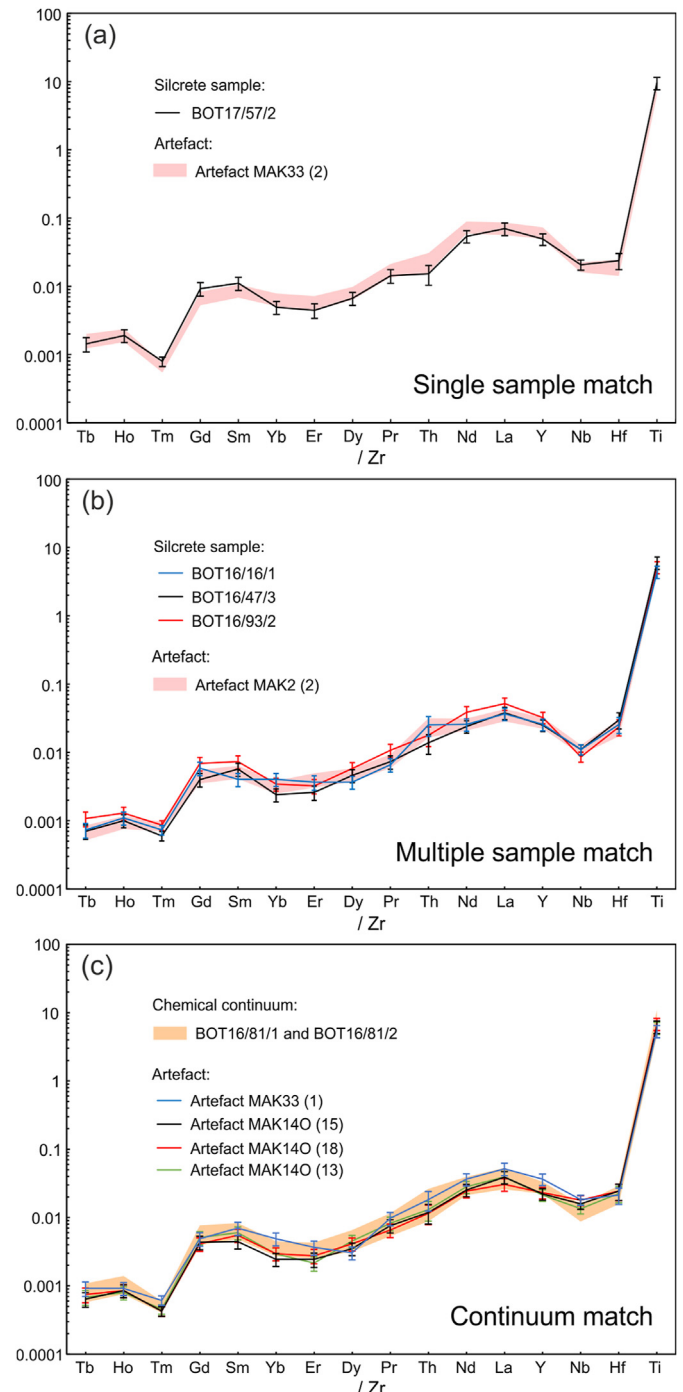


Fig. 9. Examples of permissible matches between artefacts and silcrete samples/sites. Permissible matches are shown between (a) an artefact and a single silcrete outcrop sample, (b) an artefact and multiple silcrete outcrop samples, and (c) multiple artefacts and a chemical continuum from a single site.

material provenancing, as it is based on immobile trace elements only and identifies only cases where the composition of an artefact and potential raw material source directly match within the limits of instrumentation.

Some artefacts exhibit permissible matches with single silcrete samples (Fig. 9a). In other cases, a single sample or site has the potential to be the raw material source for more than one artefact (Fig. 9c). Most commonly, however, the immobile trace element signature for an individual artefact matched that of silcrete samples (or continua) from more than one site (Fig. 9b). Following the argument made in section 5, this likely reflects silicified flood deposits with common trace element signatures being present in more than one area of the pan. Where this was the case, the petrographic properties of the artefact and silcretes from each of the raw material sites exhibiting a chemical match were compared to identify the most likely source. The properties of the silcrete raw materials were determined by direct inspection of reference samples, with artefact properties gathered by examination of high-quality images of both the individual waste flake and raw material type group from which the artefact was selected. Aspects of the petrography considered were grain size, fracture pattern, degree of cementation, level of translucence, type of cortex, the occurrence of rinds, and the presence of specks or patches of varying colour (i.e. the same properties used to define silcrete material groups during *chaîne opératoire* investigations; see section 4.2). Following the findings of Nash et al. (2016), least emphasis was placed on colour.

6.2. Sources of silcrete raw materials

Fifteen of the 46 artefacts analysed by ICP-MS/-AES can be matched to potential raw material sites on the basis of their geochemical signatures (Table 1, Fig. S1). For the 31 unmatched artefacts, it is likely that the original raw material sites were not sampled; were sampled but not analysed; or that the outcrops have been buried by aeolian or lacustrine sediment since the MSA and are no longer exposed today. Outcrop burial is most likely in pan areas where standing water occurs today, although zones of maximum flooding may have shifted over time as a result of neo-tectonic activity (see Eckardt et al., 2016).

The spatial patterns of silcrete procurement sites for each artefact are shown in Figs. 10–13. A match between an artefact and a silcrete outcrop is shown on each figure as one of four ordinal classes. These are (in descending order of confidence), cases where: (i) both the geochemistry and petrography of an artefact match those of a single sample (or samples) from a silcrete outcrop site;

(ii) both the geochemistry and petrography of an artefact match those of a chemical continuum comprising two or more silcrete samples from a site; (iii) the geochemical signature only of an artefact matches that of a sample (or samples) from a site; (iv) the geochemical signature only of an artefact matches that of a chemical continuum. The level of confidence for a match with a chemical continuum is lower than that for a single silcrete sample as the y-axis error bars for a continuum are, by definition, wider than for a single sample, hence the likelihood of a chemical match is marginally greater.

6.2.1. Raw material sources for sites MAK2 and MAK15

Two of the three artefacts analysed from site MAK2 can be matched to outcrops within Ntwetwe Pan. The assemblage from this site is small and restricted to the final stages of the *chaîne opératoire* of MSA point production. The most secure provenance is for artefact MAK2 (1) (Fig. 10), which displays chemical and petrographic matches with three single samples and one chemical continuum from sites in the northeast and south-central pan. These are all pan-marginal outcrops at elevations of c. 909–910 m asl and at straight-line distances of 15–31 km from the site. The artefact shares a geochemical signature with silcrete samples from four other sites, including one from the Boteti River; however, its petrography is different in all cases, so it is highly unlikely that the silcrete was procured from these sites. The pattern of silcrete outcrops with similar geochemical signatures on Fig. 10a suggests that the host sediments were deposited by a flood event (or events) transmitted via the Boteti River, but that the sediments were silicified to produce silcretes with differing petrographic properties in different locations. A similar interpretation can be made for other maps in Figs. 10–13 that include geochemical matches with silcrete outcrops in the Okavango system upstream of Ntwetwe. Artefact MAK2 (2) can be provenanced less securely. The artefact yields a geochemical match with three silcrete samples from the north-central and northeast of Ntwetwe Pan but matches none of these samples petrographically.

Two of the three artefacts from archaeological site MAK15 can be matched to potential raw material sources (Fig. 11). Artefact MAK15 (21) displays geochemical and petrographic matches to outcrops at c. 905–910 m asl, 25 km southeast and 42 km east of the site. The artefact also yields a chemical match with a silcrete on the Cubango River but bears no petrographic similarity. The artefact was selected from the largest raw material group (C) in this assemblage, representing flakes and tools that could have been produced from more than one silcrete block. The results for artefact

Table 1

Details of archaeological artefacts that yielded chemical matches with specific raw material sites (see Fig. S1 for images). Grid coordinate and quadrant describe the position the artefact was located within the site (see Staurset et al., 2022a, 2022b, for more details). Outlier artefacts around the excavation were surface collected and situated within an extended site grid. Raw material group indicates the silcrete type group (identified during *chaîne opératoire* analysis) from which the artefact was sampled. For full details of all artefacts analysed, see Table S1 in the Supplementary Data.

Site	Artefact number	Grid coord.	Quadrant	Level	Excavated area or outlier	Raw Material group	Description
MAK2	1	18/51	SE	Surface	Excavated area	B	Broken knapping fragment
MAK2	2	18/53	NE	Surface	Outlier	C	Flake
MAK15	20	14/49	SE	Surface	Outlier	B	Broken flake fragment
MAK15	21	11/50	NE	Surface	Excavated area	C	Broken flake fragment
MAK14K	11	15/53	NE	Surface	Excavated area	B	Broken flake fragment
MAK140	12	12/58	SE	Surface	Excavated area	A	Broken flake fragment
MAK140	13	15/58	NW	Surface	Excavated area	A	Flake
MAK140	15	11/57	NW	Surface	Excavated area	A	Broken flake fragment
MAK140	18	11/75	SE	Surface	Outlier	D	Broken flake fragment
MAK33	1	26/49	SE	Surface	Excavated area	A	Flake
MAK33	2	20/85	—	Surface	Outlier	A	Broken flake fragment
MAK33	3	36/67	SW	Surface	Excavated area	A	Flake
MAK33	8	26/71	NE	Surface	Excavated area	C	Flake
MAK33	9	12/100	SE	Surface	Excavated area	D	Flake
MAK33	24	51/107	—	Surface	Outlier	K	Flake

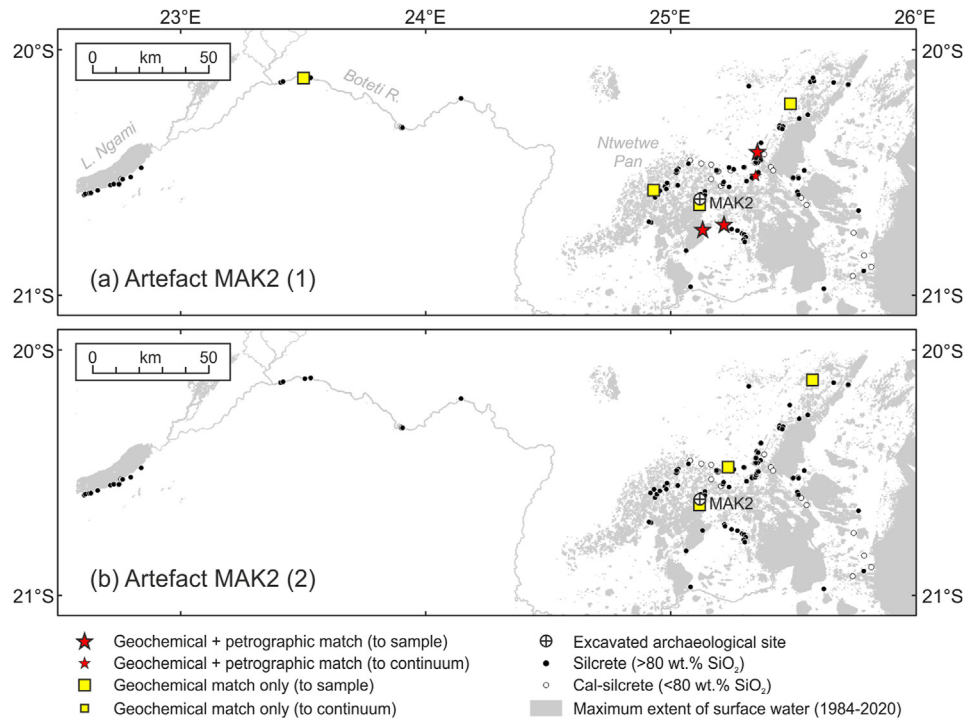


Fig. 10. Distribution of silcrete sampling sites with geochemical and petrographic matches to silcrete artefacts from archaeological site MAK2. The locations of all sites where silcrete and cal-silcrete outcrops were sampled and analysed is also shown. Details of artefacts are given in [Table 1](#) and [Table S1](#).

MAK15 (20) are less easy to interpret, with chemical matches to sites both within Ntwetwe Pan and as far west as Lake Ngami but no petrographic similarity. This artefact was selected from the second largest raw material group (B) and also represents archaeological artefacts produced from various stages of production within the *chaîne opératoire* of this silcrete type.

6.2.2. Raw material sources for sites MAK14K and MAK14O

Five of the ten artefacts from sites MAK14K and MAK14O can be matched to potential raw material sites, four securely through both geochemical and petrographic properties and one by geochemistry only. Whilst exhibiting chemical matches with outcrops as far west as Lake Ngami, the most likely provenance for artefact MAK14K (11) is an outcrop at c. 912 m asl elevation in northeast Ntwetwe, 7.5 km

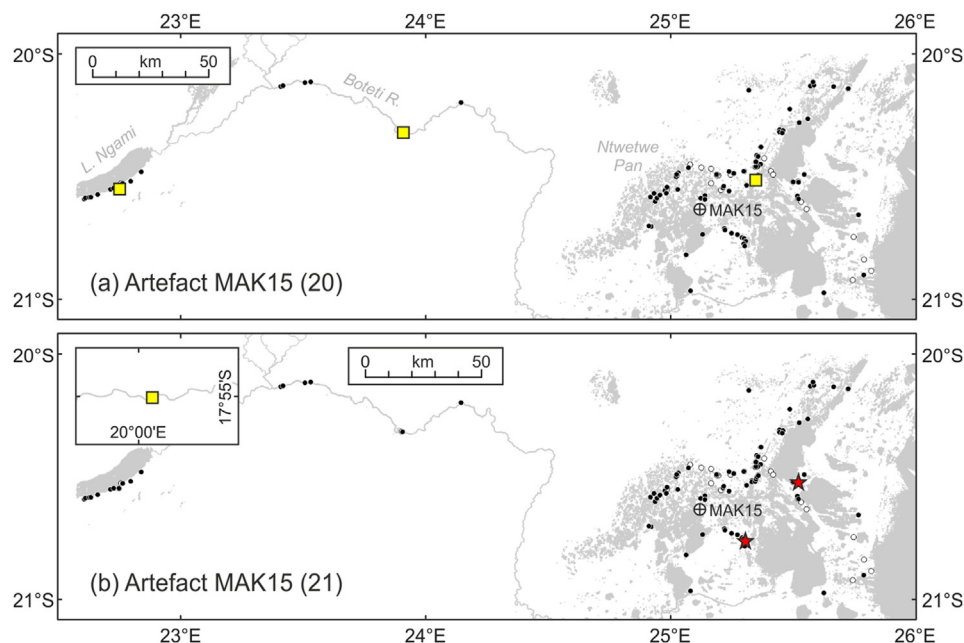


Fig. 11. Distribution of silcrete sampling sites with geochemical and petrographic matches to silcrete artefacts from archaeological site MAK15. See [Fig. 10](#) for key to symbols. Inset on panel (b) indicates a geochemical match with silcrete samples from the Cubango River in northeast Namibia (see [Fig. 1a](#) for location). Details of artefacts are given in [Table 1](#) and [Table S1](#).

northwest of the pan margin and at a straight-line distance of 55 km from the archaeological site (Fig. 12a). This artefact represents one of the smaller but most uniform of the raw material groups (B) from this assemblage, which display the characteristics of late-stage point production and tool discard.

Artefacts 12, 13 and 15 from archaeological site MAK140 can be sourced with relative confidence (Fig. 12). All are from the largest raw material group (A) from this site, which comprised several knapping sequences. These sequences illustrate lithic manufacture ranging from testing of natural silcrete blocks to the final stages of

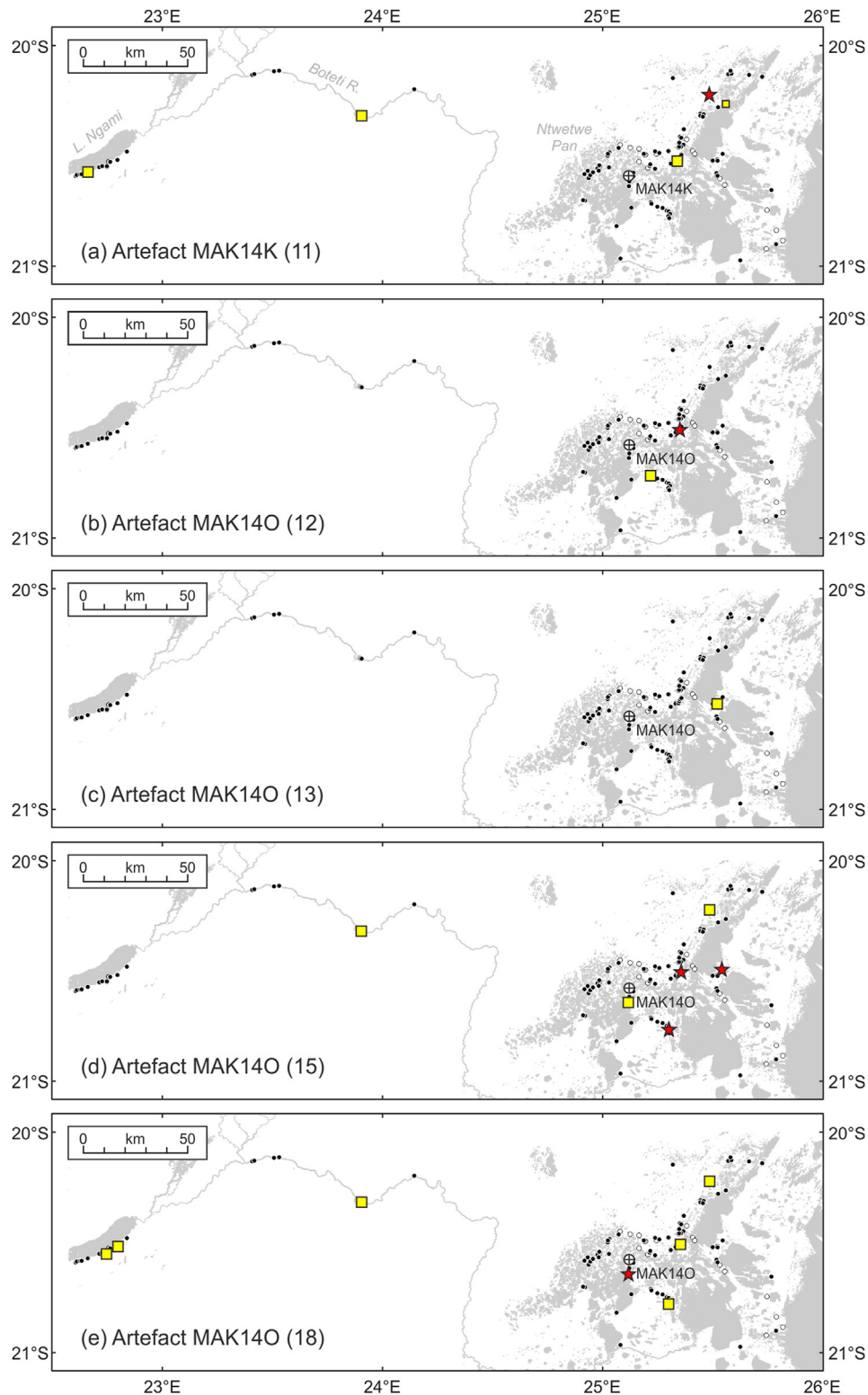


Fig. 12. Distribution of silcrete sampling sites with geochemical and petrographic matches to silcrete artefacts from archaeological sites MAK14K (a) and MAK140 (b–d). See Fig. 10 for key to symbols. Details of artefacts are given in Table 1 and Table S1.

tool production. Artefact MAK140 (15) yields geochemical and petrographic matches with silcrete samples from three outcrops at c. 911 m asl elevation and at distances of between 15 and 45 km to the southeast and east of the archaeological site. Artefact MAK140 (12) is also likely to have had a relatively local source, yielding a geochemical and petrographic match with an outcrop at c. 909 m asl and 43 km to the east. Artefact MAK140 (13) can be provenanced less securely (Fig. 12c), showing a chemical match to a single silcrete site in eastern Ntvetwe Pan but no petrographic match. The final artefact (18) is of a different raw material and from a much smaller group (D), dominated by bifacial shaping of MSA points. The geochemistry of artefact MAK140 (18) matches with silcrete samples from a wider area but shows only one chemical and petrographic match – with an outcrop at c. 908 m asl and 3.7 km due south of the archaeological site.

6.2.3. Raw material sources for site MAK33

Geochemical provenancing was proportionately least successful for site MAK33, where only six artefacts from 30 analysed could be matched to potential raw material sites (Fig. 13). Artefact MAK33 (1) yields geochemical matches with silcrete sites in the Boteti River and south-central Ntvetwe but no petrographic match with reference samples from either location. Artefact MAK33 (2) displays a geochemical and petrographic match with a silcrete outcrop 25 km to south of the site at c. 902 m asl. Artefact MAK33 (3)

displays geochemical matches with silcrete sites on the Cubango River and in north-central Ntvetwe but no petrographic match. These three matches are all from the large raw material group (A), which was dominated by Levallois production. This group contains a number of tabular refitted silcrete blocks that are 10–15 cm in diameter and would have weighed in excess of 1 kg. However, the group also includes a number of blanks that are of this size, indicating they were produced from even larger cores. These blanks could have been produced elsewhere and brought to MAK33 ready-made, or manufactured on site and discarded, while the core was carried away when the site was abandoned. End-products in this raw material include unifacial and bifacial points as well as elongated scrapers of 10–15 cm length.

Artefact MAK33 (8) produces geochemical matches with multiple samples from a site on the Cubango River but no petrographic match to any of these samples (Fig. 13d). This artefact is from raw material group (C), which is a very uniform small group comprising core cleaning debris that likely represents the outer rind of a core from either group A or B. A geochemical match is obtained between artefact MAK33 (9) and two outcrops at 12 km east and 25 km NNE of the archaeological site. The petrography of the artefact and reference samples are different but the identification of two chemical matches in the same part of the pan suggests the silcrete may have originated in this broad area. Artefact MAK33 (9) is from raw material group D, a distinctive fully refitted tabular block of

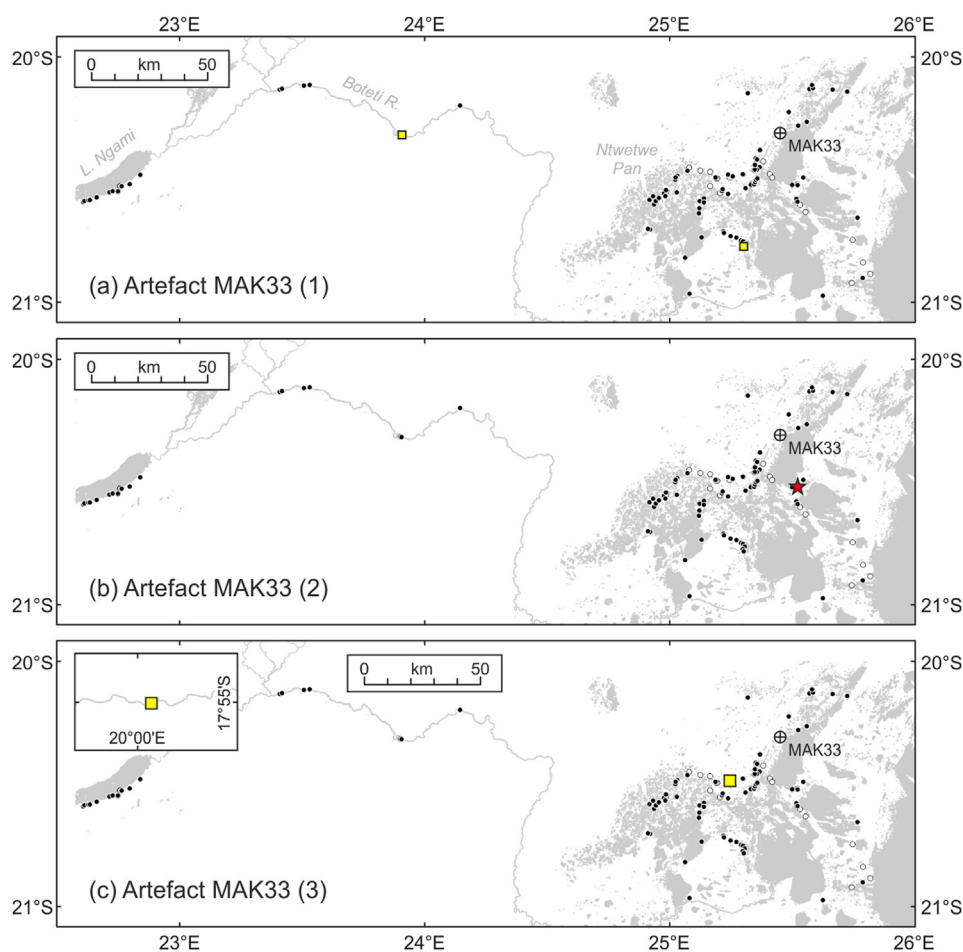


Fig. 13. Distribution of silcrete sampling sites with geochemical and petrographic matches to silcrete artefacts from archaeological site MAK33. See Fig. 10 for key to symbols. Inset on panels (c) and (d) indicates a geochemical match with silcrete samples from the Cubango River in northeast Namibia (see Fig. 1a for location). Details of artefacts are given in Table 1 and Table S1.

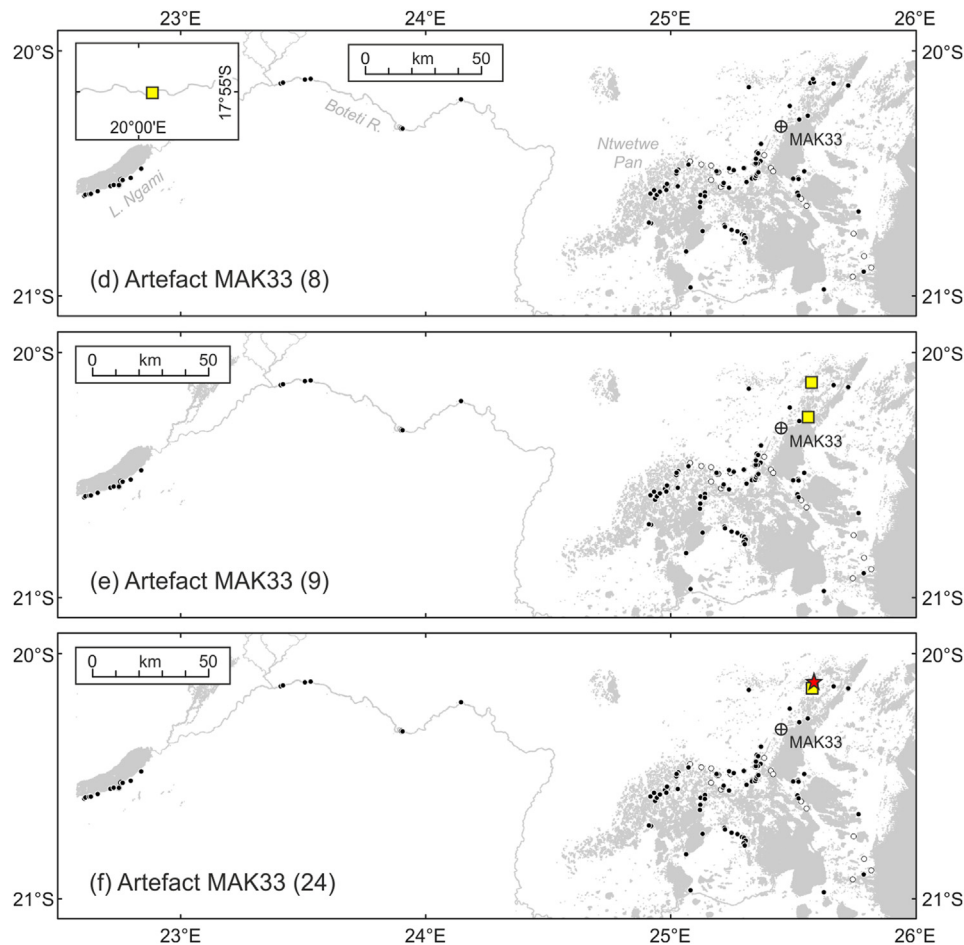


Fig. 13. (continued).

silcrete used to manufacture elongated blanks. The distribution of group D is confined to the South concentration on this site (Staurset et al., 2022b). The artefact was retrieved from the middle of this concentration and is the firmest attribution to a specific archaeological raw material group in this study. Finally, artefact MAK33 (24) can be sourced more securely, displaying both geochemical and petrographic matches with a single silcrete outcrop at c. 920 m asl situated 25 km northeast of the site plus a geochemical match only with an outcrop 24 km to the northeast of the site. This artefact is from raw material group K, and represents a very distinct type of silcrete that normally appears on site as thin, well-cemented, 10–15 cm diameter, flat slabs. These slabs served as natural blanks for the production of bifacial points and are found in various states of manufacture in all the working areas of MAK33 (Staurset et al., 2022b).

7. Discussion

7.1. Archaeological implications

The distances involved in the acquisition of lithic raw materials across a landscape have important implications for determining the foraging patterns and ranges of early humans, and their resource selection preferences (e.g. Ambrose, 2006; Minichillo, 2006; Thompson et al., 2010; Wilkins, 2017; Will, 2021; Mackay et al., 2022). Whilst recognising the limits imposed by sampling and the present-day exposure of silcrete outcrops, the collective results

in Figs. 10–13 suggest that the MSA populations that utilised Ntswetwe Pan obtained silcrete for stone tool manufacture from local sources within the pan, ranging from 7 to 55 km distant. They did so during dry or seasonally dry periods, when water levels within the Makgadikgadi Pans complex were low. This assertion is supported by OSL dating of site MAK14K, where the window for site usage (centred on c.72 ka) falls just before a high-stand in the reconstructed lake-level curve for the Makgadikgadi system (see Burrough et al., 2009; de Cort et al., 2021; Burrough et al., 2022). Further, all five archaeological sites, and all of the most securely provenanced silcrete sources (i.e. those with both geochemical and petrographic matches to specific locations on Figs. 10–13), are situated at 920 m asl or lower. All would therefore be 10s of metres underwater during the various Makgadikgadi megalake phases, even allowing for subtle neotectonic movements (Cooke and Versteppen, 1984; Shaw et al., 1992; Ringrose et al., 2005; Burrough et al., 2007, 2009; Burrough and Thomas, 2008; Schmidt et al., 2017).

Our use of the term ‘local’ to describe the relatively far-ranging site-to-source foraging patterns shown in Figs. 10–13 may appear at odds with other southern African MSA investigations. Thompson et al. (2010) and Will (2021), for example, both set a limit of <10 km for local procurement vs. a non-local range of >10 km (Will, 2021) or alternatively >25–50 km (Minichillo, 2006; Brooks et al., 2018). However, as Ambrose (2006) has argued, any single definition of ‘local vs. non-local’ is unlikely to be applicable for all environmental settings. The expanded local foraging range proposed here is

justified by the relative ease of access to silcrete resources within Ntswetwe Pan – all outcrops are located either on, or close to, a flat lake basin floor – and is further supported by previous results from northwest Botswana, where non-local acquisition of silcrete during the MSA involved transport distances of up to 295 km (Nash et al., 2013, 2016).

Plotting the results for the most securely provenanced artefacts reveals further information about foraging patterns and behaviours on Ntswetwe Pan during the MSA (Fig. 14). Four of the five excavated open-air sites (MAK2, MAK14K, MAK14O, MAK15) are located in the central pan. For these sites, the most securely identified silcrete sources are located up to 55 km to the northeast, east or southeast. The remaining site (MAK33) is in northeastern Ntswetwe, where silcrete was likely sourced from c. 25 km to the northeast and southeast. As Fig. 14 shows, many of the securely identified silcrete sources are clustered in south-central and eastern sectors of the pan; this suggests a preference for silcretes from particular areas. As the five excavated sites were likely occupied at different times during the MSA (see section 3 and Burrough et al., 2022), this resource preference may have been a longer-term behavioural feature of populations in the Ntswetwe region.

Combining the results of geochemical and petrographic provenancing with *chaîne opératoire* analysis of lithic materials from the five excavated sites (reported in Staurset et al., 2022a,b) confirms that the transport of silcrete from specific outcrops was an inherent feature of MSA lithic tool production on Ntswetwe Pan. Blocks of silcrete (in some cases >15 cm diameter) were carried to sites, where they were fully knapped (e.g. at sites MAK33 and to an extent MAK14O), partially worked and taken elsewhere (e.g. MAK14O, MAK33), or in some instances simply abandoned (e.g. MAK14O, MAK33). At sites MAK2, MAK14K and MAK15, earlier stages of tool production were executed prior to arrival at the site. There is, however, little evidence in the field that initial cleaning of blocks or preparation of cores was undertaken at the source locations. As noted in section 3, tool production on all sites was largely

confined to the production of MSA points. Lithic analyses in Staurset et al. (2022a,b) suggest that individual toolmakers were stringent in their requirements of what constituted a 'suitable' blank or tool, and confirm that transporting raw material tens of kilometres did not appear to influence a toolmaker's requirements for anything less than 'perfect' products. All five excavated sites are short-term single-use occupations. It is therefore unlikely that the silcrete blocks transported only to be abandoned on-site were being cached in preparation for future use. The movement of substantial weights of raw material over considerable distances is known archaeologically (e.g. Brooks et al., 2018; Karlin and Julien, 2019; Mackay et al., 2022). However, the foraging pattern identified on Ntswetwe, characterised by the transport of raw materials to relatively distant tool manufacturing locations, indicates more energy expenditure and a greater range of movement than is normal for 'local' procurement (see also Mackay et al., 2022, for a similar conclusion).

The local silcrete procurement pattern identified at the five excavated archaeological sites is indicative of the wider strategy for stone acquisition used by MSA populations in Ntswetwe Pan. The five sites are representative of the >100 exposed open-air MSA sites documented during surveys of the lake basin floor (see Coulson et al., 2022; Staurset et al., 2022a). A characteristic of lithics at all the recorded open-air MSA sites is the dominance of dark grey to black silcrete. Artefacts manufactured from the petrographically distinct silcrete found along the upper Boteti River and around Lake Ngami – the next closest major areas of silcrete outcrop beyond Ntswetwe – were not identified at any of the sites. Further, there were no indications of what are often referred to in the archaeological literature as 'exotic' non-local materials (e.g. Ambrose, 2002; Beaumont and Vogel, 2006; Minichillo, 2006; Brooks et al., 2018). Pebbles of brightly-coloured fine-grained cherts are documented at Later Stone Age sites in the north- and south-central areas of Ntswetwe (see Coulson et al., 2022). Imported exotic raw materials are also documented in the MSA levels of White Painting Shelter

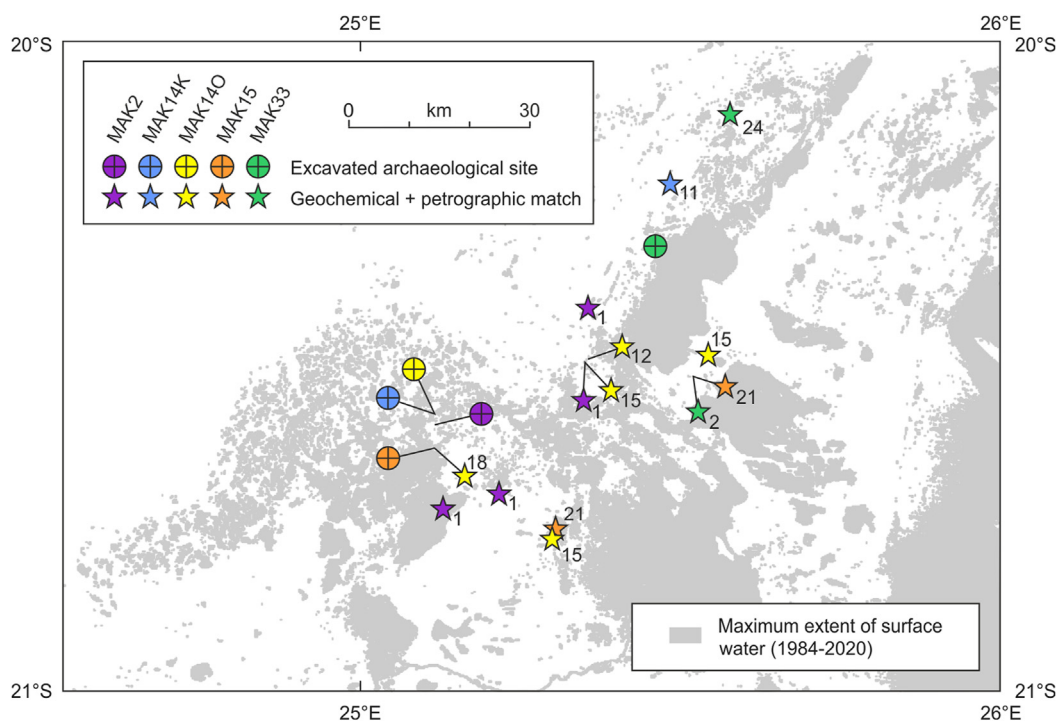


Fig. 14. Combined provenancing results for artefacts with both geochemical and petrographic matches from all archaeological sites. Numbers next to symbols match the numbering system used in Figs. 10–13.

(Robbins et al., 2000) and Rhino Cave (Coulson et al., 2011) in the Tsodilo Hills, northwest Botswana (Fig. 1a). However, local dark grey and black silcrete appears to have been the material of choice for tool manufacture on Ntwetwe Pan during the MSA.

Although this study is limited to the acquisition of lithic raw materials during the MSA, it can be argued that Ntwetwe Pan – as part of the Makgadikgadi Pans complex – is a resource-rich area. Unlike other regions of the Middle Kalahari, silcrete is readily available over a large area, making it a reliable resource. Additionally, as today, the lake basin floor would have provided not only fresh water but also an abundance of game and plant resources. However, easily accessible shelter is not available, which may account for the lack of any indication of long-term or repeat occupation of sites. Our results can be compared to earlier research in the Tsodilo Hills, another resource-rich environment (Robbins et al., 2000; Nash et al., 2013). While there is a lack of locally available silcrete at Tsodilo (it was instead obtained by long-distance acquisition), quartz, quartzite and rock crystal are abundant. Again, fresh water, game and plant resources are readily available. In addition, the Hills contain numerous caves and rockshelters, with evidence of long-term occupation and affording the possibility of repeat visits. As stated by Ambrose (2012), if resources are predictable and dense, then hunter-gatherers are likely to have small, defended home ranges and minimal intergroup interactions, including infrequent exchange of materials and information (see also Grove, 2009). However, our investigations show that MSA populations in two different resource-rich areas of the Kalahari behaved in very different ways with regard to stone procurement. This implies that a more nuanced approach is needed when defining the size of an MSA home range, particularly in relation to lithic raw material preference and transport.

The pattern of short-term site usage in this study indicates expedient raw material acquisition, perhaps concurrent with other foraging activities. A number of scenarios could account for the patterns of silcrete acquisition in relation to site locations. For example, procurement from an easterly quadrant at the four sites in central Ntwetwe could reflect a cultural behaviour (i.e. foraging to the east, moving broadly westwards across the pan, stopping for a short period of time to produce tools in the central areas, and then moving on; see Fig. 14). Silcrete procurement from the northeast and southeast at the largest site, MAK33, could hint at a petal-like pattern of foraging movement from the site during its period of use. Alternatively, it could be that slabs of the thin, fine-grained, tabular silcrete used to make artefact MAK33 (24) were already being transported when the large block of black silcrete used to produce artefact MAK33 (2) was collected and moved to the site. It is worth repeating that the 'tidiness' and relatively undisturbed nature of site MAK33 supports an interpretation of short-term and single-use occupation (see section 3).

In summary, the distinctive patterns of local raw material selection seen on Ntwetwe Pan appear to be the result of purposeful, culturally-mediated choices (see Thomas et al., 2022, for further discussion). The absence of silcrete from the Boteti River and Lake Ngami – used extensively for tool manufacture by the populations that occupied MSA sites in the Tsodilo Hills – may hint that forager movement between Ntwetwe Pan and areas further west was limited. Within the limits of our data, we know that MSA populations on Ntwetwe Pan did not venture west of the pan to acquire silcrete. However, before claims of behaviours such as territoriality can be made, it is necessary to test if any of the silcrete artefacts from the Tsodilo MSA sites that could not be provenanced in Nash et al. (2013, 2016) were obtained from Ntwetwe Pan. This will be the subject of a future study.

7.2. Methodological advances

7.2.1. Advances in geochemical provenancing

The immobile trace element signature-based approach used here to determine lithic raw material sources has identified the provenance of c. 33% of the silcrete artefacts analysed. This compares with success rates of up to 71% for silcrete artefacts from MSA sites in northwest Botswana using a more traditional statistical approach (Nash et al., 2013, 2016). The lower proportion of matches in this study could, in part, be a product of the new method – we will test this in a future study by applying our approach to existing datasets – but is also likely to reflect the complex geomorphic environment of Ntwetwe Pan. The low success rates at site MAK33 compared to sites in the central pan could, for example, relate to the configuration of the lake system at the time that MAK33 was in use. As Burrough et al. (2022) identify, the landscape to the west of site MAK33 is covered by aeolian sediments that have accumulated since the site was formed, while the area to the east and southeast has experienced lacustrine sedimentation; it is possible therefore that outcrops that were exploited during the MSA are now buried. The context is different for outcrops in the central and southern pan – these are in a net deflation zone, meaning that silcrete sources are more likely to have remained exposed.

Regardless of their explanation, the lower success rates in this study mean there are fewer data points to work with in terms of understanding silcrete acquisition patterns and hence movement within a foraging range. We would argue, however, that the results presented here are more robust than using a purely statistical approach. Traditional statistical approaches to stone provenancing incorporate two levels of uncertainty – analytical uncertainty associated with the determination of element concentrations, and statistical uncertainty associated with the attribution of an artefact to a potential raw material source. The only statistical inference in the approach used in this study is that introduced to account for analytical uncertainty (see section 6.1). Unlike traditional statistical approaches, there is no possibility in our method for concentrations of one chemical element to fall just outside statistical confidence intervals while the majority of other elements are within limits – either the immobile trace element signature for an artefact matches the signature for a source within analytical error for all selected elements or it doesn't. In addition, geochemical matches are supplemented by petrographic analyses to identify the most secure source, thus respecting both the geochemical and petrographic integrity of the raw material.

The results presented here illustrate the importance of analysing multiple samples from individual outcrops or scatters when attempting to source provenance silcretes. Individual silcrete outcrops in Ntwetwe Pan have inherited the geochemical complexity of the sediment sequences within which they formed, such that multiple geochemical signatures may be exhibited across samples from a single site. The same will be true of any silcrete developed within lacustrine or fluvial host sediments in areas with complex underlying geology. At the very least, we would recommend taking multiple analyses down a vertical silcrete outcrop to test for chemical homogeneity at the profile scale before proceeding with sampling.

7.2.2. Archaeological advances

This study represents the first time that geochemical fingerprinting has been combined with *chaîne opératoire* analysis for any newly and fully excavated MSA site in southern Africa. Previous silcrete provenancing investigations in Botswana have analysed artefact collections from sites in the Tsodilo Hills that were partially excavated some time previously, and sites such as #Gi (Fig. 1a)

where only samples of the assemblage were retained initially and/or are now available (see Nash et al., 2013, 2016). The process of artefact selection is critical in connecting the archaeological assemblage to the geochemical analysis. For this study, assemblages were separated into silcrete raw material types, with refitting used to refine these type groups to obtain the greatest confidence that the artefacts selected for analysis were representative of particular blocks of material – the greater the number of pieces refitted from the same raw material type group, the greater the certainty in the coherence of that group, and the greater the likelihood that a sampled artefact is representative of that group.

For this study, only artefacts that were representative of silcrete type groups – rather than refitted pieces – were selected for geochemical analysis. Our goal for future provenancing work will be to select pieces from *within* refitted blocks for analysis, as this will maximise the potential for archaeological interpretation. That may, however, be some time away since it will require high level permissions and the archaeologist's justification that the process warrants the destruction of an artefact. As geochemical provenancing methods progress and the minimum sample size required for trace element detection by ICP-MS decreases, this will be the optimal approach.

8. Conclusions

This study has combined the use of silcrete provenancing and *chaîne opératoire* analysis to explore patterns of lithic raw material procurement, and hence mobility, at five open-air MSA sites in Ntswetwe Pan. Our results indicate that the groups that utilised these short-term single-use sites obtained silcrete for tool manufacture from sources within the pan, 7–55 km distant. OSL dating indicates that site occupancy, and hence the movement of raw materials, took place during dry or seasonally dry periods when water levels within the Makgadikgadi Pans complex were low. The simultaneous analysis of multiple MSA sites has allowed us to identify silcrete source areas common to more than one site, suggesting a preference for silcrete from particular locations that may have been a longer-term behavioural feature of MSA populations in the Ntswetwe region. The distances over which silcrete was transported in Ntswetwe are smaller than identified in previous investigations at similar aged MSA sites in northwest Botswana. Both Ntswetwe and northwest Botswana are relatively rich in stone, water, animal and plant resources. The difference in silcrete procurement ranges in the two regions may be related to silcrete availability and/or raw material preference, but this requires further investigation.

This study has also made methodological advances that will benefit future source provenancing efforts, particularly for sites where silcrete was the primary material used for tool manufacture. First, our geochemical fingerprinting approach focusses only upon immobile trace elements within silcretes. Second, rather than rely upon statistical inference, we directly compare the immobile trace element signatures of silcrete artefacts against equivalent signatures for sources, with the results supplemented by petrographic comparisons. Third, the artefacts chosen for chemical assay are selected as part of a *chaîne opératoire* analysis of the full assemblage of lithics from a fully excavated site, allowing us to draw more powerful inferences about human behaviour than random sampling of artefacts could achieve. Finally, our data highlight the sedimentary and geochemical complexity of silcretes developed in large ephemeral lake basins such as Ntswetwe Pan, fed by river catchments that drain areas of complex geology. We would urge all future silcrete provenancing investigations to test the chemical homogeneity of individual profiles prior to embarking on any sampling campaign.

Funding statement

This research was funded by Research Project Grant RPG-2015-344 awarded by The Leverhulme Trust. Additional funding and aid were gratefully received from the University of Oxford, University of Brighton, University of Botswana, University of Oslo and Norsk Arkeologisk Selskap.

Author contributions

DJN, DSGT, SLB and SDC conceived the original study and secured funding. TJRC and DJN conducted the analysis of immobile trace element signatures. SS was responsible for the selection of archaeological waste flakes for geochemical analysis. DJN, DSGT and SM were responsible for sampling of silcrete raw material sites. DJN led the overall manuscript development. All authors contributed to the preparation of the final manuscript.

Declaration of competing interest

The authors declare that they have no known competing financial interests or personal relationships that could have appeared to influence the work reported in this paper.

Data availability

The full data sets for this investigation, including analyses of Certified Reference Materials, are available from the Brighton Research Data repository at <https://doi.org/10.17033/DATA.00000286>.

Acknowledgements

Field and museum-based research took place under research permit EWT 8/36/4 XXXV (9), issued 22 April 2016 by the Botswana Ministry of Environment, Wildlife and Tourism (ref EWT 8/36/4 XXXV (52)), extended on 29 June 2018 by the Botswana Ministry of Environment, Natural Resources, Conservation and Tourism (ref ENT 8/36/4 XXXXII (43)). Artefacts were shipped to Europe under export permits issued by the Botswana Ministry of Environment, Wildlife and Tourism. Fieldwork in 2011 was carried out under research permit ref EWT 8/36/4 XV (25), as detailed in Nash et al. (2013). Thanks to Uncharted Africa, Gweta Lodge and Eric Walker for logistical support during fieldwork and to ALS Minerals for geochemical analyses. We acknowledge the continued support of the National Museum of Botswana for laboratory space and the loan of equipment. Most of all, we express our gratitude to University of Botswana students Oratile Ramore, Catherine Legabe, Jane Masisi, Topo Mpho Chengeta, Casper Lekgetho and Agang Motlaleng for their contributions to archaeological fieldwork in Ntswetwe Pan. We would like to thank two anonymous reviewers for their positive and helpful suggestions to improve the manuscript.

Appendix A. Supplementary data

Supplementary data to this article can be found online at <https://doi.org/10.1016/j.quascirev.2022.107811>.

References

- Alley, N.F., 1998. Cainozoic stratigraphy, palaeoenvironments and geological evolution of the Lake Eyre Basin. *Palaeogeogr. Palaeoclimatol. Palaeoecol.* 144, 239–263.
- Ambrose, S.H., 2002. Small things remembered: Origins of early microlithic industries in Sub-Saharan Africa. In: Kuhn, S.L., Elston, R.G. (Eds.), *Thinking Small: Global Perspectives on Microlithization*, vol. 12. Archaeological Papers of the

- American Anthropological Association, pp. 9–29.
- Ambrose, S.H., 2006. Howiesons Poort lithic raw material procurement patterns and the evolution of modern human behavior: a response to Minichillo (2006). *J. Hum. Evol.* 50, 365–369.
- Ambrose, S.H., 2012. Obsidian dating and source exploitation studies in Africa: Implications for the evolution of human behavior. In: Liritzis, I., Stevenson, C.M. (Eds.), *Obsidian and Ancient Manufactured Glasses*. University of New Mexico Press, Albuquerque, pp. 56–72.
- Andrefsky, W.A.J., 1994. Raw-material availability and the organization of technology. *Am. Antiq.* 59, 21–34.
- Armenteros, I., Bustillo, M.A., Blanco, J.A., 1995. Pedogenic and groundwater processes in a closed Miocene basin (Northern Spain). *Sediment. Geol.* 99, 17–36.
- Aubry, T., Luis, L., Mangado Llach, J., Matias, H., 2012. We will be known by the tracks we leave behind: Exotic lithic raw materials, mobility and social networking among the Côa Valley foragers (Portugal). *J. Anthropol. Archaeol.* 31, 528–550.
- Baillieu, T.A., 1979. Makgadikgadi pans complex of central Botswana. *Geol. Soc. Am. Bull.* 90, 289–312.
- Bamforth, D.B., 1991. Technological organization and hunter-gatherer land use: A California example. *Am. Antiq.* 56, 216–234.
- Beaumont, P.B., Vogel, J.C., 2006. On a timescale for the past million years of human history in central South Africa. *South Afr. J. Sci.* 102, 217–228.
- Bhalotra, Y.P.R., 1987. Climate of Botswana, Part II: Elements of Climate. Meteorological Services, Gaborone.
- Bhatia, M.R., Crook, K.A.W., 1986. Trace element characteristics of graywackes and tectonic setting discrimination of sedimentary basins. *Contrib. Mineral. Petrol.* 92, 181–193.
- Bolhar, R., Woodhead, J.D., Hergt, J.M., 2003. Continental setting inferred for emplacement of the 2.9–2.7 Ga Belingwe Greenstone Belt, Zimbabwe. *Geology* 31, 295–298.
- Boocock, C., van Straten, O.J., 1962. Notes on the geology and hydrogeology of the Central Kalahari region, Bechuanaland Protectorate. *Trans. Geol. Soc. S. Afr.* 65, 125–171.
- Brooks, A.S., Yellen, J.E., Potts, R., Behrensmeyer, A.K., Deino, A.L., Leslie, D.E., Ambrose, S.H., Ferguson, J.R., d'Errico, F., Zipkin, A.M., 2018. Long-distance stone transport and pigment use in the earliest Middle Stone Age. *Science* 360, 90–94.
- Brown, K.S., 2011. The Sword in the Stone: Lithic Raw Material Exploitation in the Middle Stone Age at Pinnacle Point Site 5–6, Southern Cape, South Africa. Unpublished PhD Thesis. Department of Archaeology, University of Cape Town.
- Burrough, S.L., 2022. The Makgadikgadi basin. In: Eckardt, F. (Ed.), *Landscapes and Landforms of Botswana*. Springer Nature, Heidelberg, pp. 77–90.
- Burrough, S.L., Thomas, D.S.G., 2008. Late Quaternary lake-level fluctuations in the Mababe Depression: Middle Kalahari palaeolakes and the role of Zambezi inflows. *Quat. Res.* 69, 388–403.
- Burrough, S.L., Thomas, D.S.G., Shaw, P.A., Bailey, R.M., 2007. Multiphase Quaternary highstands at Lake Ngami, Kalahari, northern Botswana. *Palaeogeogr. Palaeoclimatol. Palaeoecol.* 253, 280–299.
- Burrough, S.L., Thomas, D.S.G., Singarayer, J.S., 2009. Late Quaternary hydrological dynamics in the Middle Kalahari: Forcing and feedbacks. *Earth Sci. Rev.* 96, 313–326.
- Burrough, S.L., Thomas, D.S.G., Allin, J.T., Coulson, S.D., Mothulatsipi, S., Nash, D.J., Staurset, S., 2022. Lessons from a lake bed: Unpicking hydrological change and early human landscape use in the southern African interior. *Quat. Sci. Rev.* 291, 107662. <https://doi.org/10.1016/j.quascirev.2022.107662>. In this issue.
- Bustillo, M.A., Bustillo, M., 1993. Rhythmic lacustrine sequences with silcretes from the Madrid Basin, Spain: Geochemical trends. *Chem. Geol.* 107, 229–232.
- Bustillo, M.A., Bustillo, M., 2000. Miocene silcretes in argillaceous playa deposits, Madrid Basin, Spain: Petrological and geochemical features. *Sedimentology* 47, 1023–1037.
- Carney, J.N., Aldiss, D.T., Lock, N.P., 1994. The Geology of Botswana (Bulletin 37). Geological Survey Department, Botswana, Lobatse.
- Celli, N.L., Lebedev, S., Schaeffer, A.J., Gaina, C., 2020. African cratonic lithosphere carved by mantle plumes. *Nat. Commun.* 11, 92. <https://doi.org/10.1038/s41467-019-13871-2>.
- Clark, A.E., 2017. From activity areas to occupational histories: New methods to document the formation of spatial structure in hunter-gatherer sites. *J. Archaeol. Method Theor* 24, 1300–1325.
- Cochrane, G.W.G., Webb, J.A., Doelman, T., Habgood, P.J., 2017. Elemental differences: Geochemical identification of aboriginal silcrete sources in the Arcadia Valley, eastern Australia. *J. Archaeol. Sci. Reports* 15, 570–577.
- Cooke, H.J., 1980. Landform evolution in the context of climatic change and neotectonism in the Middle Kalahari of north central Botswana. *Trans. Inst. Br. Geogr.* 5, 80–99.
- Cooke, H.J., Verstappen, B.T., 1984. The landforms of the western Makgadikgadi Basin of northern Botswana. *Z. Geomorphol.* 28, 1–19.
- Coulson, S., Staurset, S., Walker, N.J., 2011. Ritualized behavior in the Middle Stone Age: Evidence from Rhino cave, Tsodilo Hills, Botswana. *PaleoAnthropology* 2011, 18–61.
- Coulson, S.D., Staurset, S., Mothulatsipi, S., Burrough, S.L., Nash, D.J., Thomas, D.S.G., 2022. Thriving in the Thirstland: New Stone Age sites from the Middle Kalahari, Botswana. *Quat. Sci. Rev.* 107695. <https://doi.org/10.1016/j.quascirev.2022.107695>. In this issue.
- de Cort, G., Chevalier, M., Burrough, S.L., Chen, C.Y., Harrison, S.P., 2021. An uncertainty-focused database approach to extract spatiotemporal trends from qualitative and discontinuous lake-status histories. *Quat. Sci. Rev.* 258. <https://doi.org/10.1016/j.quascirev.2021.106870>.
- de Vries, J.J., Selaolo, E.T., Beekman, H.E., 2000. Groundwater recharge in the Kalahari, with reference to paleo-hydrologic conditions. *J. Hydrol.* 238, 110–123.
- de Wit, M.J., Linol, B., Furnes, H., Muedi, T., Valashiya, K., 2020. Pillow talk: Volcanic rocks of the Karoo that formed many leagues under the Gondwanan sea. *S. Afr. J. Geol.* 123, 297–330.
- Dietl, H., Kandel, A.W., Conard, N.J., 2005. Middle Stone Age settlement and land use at the open-air sites of Geelbek and Anyskop, South Africa. *J. Afr. Archaeol.* 3, 231–242.
- Eckardt, F.D., Bryant, R.G., McCulloch, G.P., Spiro, B.F., Wood, W.W., 2008. The hydrochemistry of a semi-arid pan basin case study: Sua Pan, Makgadikgadi, Botswana. *Appl. Geochem.* 23, 1563–1580.
- Eckardt, F.D., Cotterill, F.P.D., Flügel, T.J., Kahle, B., McFarlane, M.J., Rowe, C., 2016. Mapping the surface geomorphology of the Makgadikgadi Rift Zone (MRZ). *Quat. Int.* 404, 115–120.
- Enloe, J.G., 2004. Equifinality, assemblage integrity and behavioral inferences at Verberie. *J. Taphonomy* 2, 147–165.
- Eren, M.I., Diez-Martin, F., Dominguez-Rodrigo, M., 2013. An empirical test of the relative frequency of bipolar reduction in Beds VI, V, and III at Mumba Rock-shelter, Tanzania: Implications for the East African Middle to Late Stone Age transition. *J. Archaeol. Sci.* 40, 248–256.
- Franchi, F., Kelepile, T., Di Capua, A., De Wit, M.C.J., Kemiso, O., Lasarwe, R., Catuneanu, O., 2021. Lithostratigraphy, sedimentary petrography and geochemistry of the Upper Karoo Supergroup in the central Kalahari Karoo Sub-Basin, Botswana. *J. Afr. Earth Sci.* 173. <https://doi.org/10.1016/j.jafrearsci.2020.104025>.
- Galerne, C.Y., Neumann, E.R., Planke, S., 2008. Emplacement mechanisms of sill complexes: Information from the geochemical architecture of the Golden Valley Sill Complex, South Africa. *J. Volcanol. Geoth. Res.* 177, 425–440.
- Greaney, A.T., Rudnick, R.L., Gaschnig, R.M., Whalen, J.B., Luais, B., Clemens, J.D., 2018. Geochemistry of molybdenum in the continental crust. *Geochim. Cosmochim. Acta* 238, 36–54.
- Grove, M., 2009. Hunter-gatherer movement patterns: Causes and constraints. *J. Anthropol. Archaeol.* 28, 222–233.
- Haddon, I.G., McCarthy, T.S., 2005. The Mesozoic-Cenozoic interior sag basins of Central Africa: The Late-Cretaceous-Cenozoic Kalahari and Okavango basins. *J. Afr. Earth Sci.* 43, 316–333.
- Helgren, D.M., 1984. Historical geomorphology and geoarchaeology in the southwestern Makgadikgadi Basin, Botswana. *Ann. Assoc. Am. Geogr.* 74, 298–307.
- Jourdan, F., Bertrand, H., Scharer, U., Blichert-Toft, J., Feraud, G., Kampunzu, A.B., 2007. Major and trace element and Sr, Nd, Hf and Pb isotope compositions of the Karoo large igneous province, Botswana-Zimbabwe: Lithosphere vs mantle plume contribution. *J. Petrol.* 48, 1043–1077.
- Julien, M., Karlin, C., 2015. Un automne à Pincevent. Le campement magdalénien du niveau IV20. *Les Nouvelles de l'archéologie*, pp. 5–11.
- Kamenetsky, V.S., Maas, R., Kamenetsky, M.B., Yaxley, G.M., Ehrig, K., Zellmer, G.F., Bindeman, I.N., Sobolev, A.V., Kuzmin, D.V., Ivanov, A.V., Woodhead, J., Schilling, J.G., 2017. Multiple mantle sources of continental magmatism: Insights from “high-Ti” picrites of Karoo and other large igneous provinces. *Chem. Geol.* 455, 22–31.
- Kampunzu, A.B., Tombale, A.R., Zhai, M., Bagai, Z., Majaule, T., Modisi, M.P., 2003. Major and trace element geochemistry of plutonic rocks from Francistown, NE Botswana: evidence for a Neoproterozoic continental active margin in the Zimbabwe craton. *Lithos* 71, 431–460.
- Karlin, C., Julien, M., 2019. An autumn at Pincevent (Seine-et-Marne, France): Refitting for an ethnographic approach of a Magdalenian settlement. *Archaeol. Anthropol. Sci.* 11, 4437–4465.
- Key, R.M., Ayres, N., 2000. The 1998 edition of the National Geological Map of Botswana. *J. Afr. Earth Sci.* 30, 427–451.
- Kot, M., Pavlenok, K., Krajcarz, M.T., Pavlenok, G., Shneider, S., Khudjanazarov, M., Leloch, M., Szymczak, K., 2020. Raw material procurement as a crucial factor determining knapping technology in the Katta Sai complex of Middle Palaeolithic sites in the western Tian Shan piedmonts of Uzbekistan. *Quat. Int.* 559, 97–109.
- Kurpiel, R., Pickering, R., Maas, R., Stern, N., 2019. Lead (Pb) isotope signatures for silcrete sources from the Willandra Lakes region, Australia: A pilot study of a new method for provenancing silcrete artefacts. *J. Archaeol. Sci. Reports* 23, 62–71.
- Lekula, M., Lubczynski, M.W., Shemang, E.M., 2018. Hydrogeological conceptual model of large and complex sedimentary aquifer systems – Central Kalahari Basin. *Phys. Chem. Earth, Parts A/B/C* 106, 47–62.
- Mackay, A., Ames, C.J.H., McNeil, J.-L., Shaw, M., 2022. Reconstructing Middle Stone Age mobility patterns from raw material transfers in South Africa's Still Bay (77–70 ka) technocomplex. *Archaeol. Anthropol. Sci.* 14, 14. <https://doi.org/10.1007/s12520-021-01484-0>.
- Maier, W.D., Rasmussen, B., Fletcher, I.R., Godel, B., Barnes, S.J., Fisher, L.A., Yang, S.H., Huhma, H., Lahaye, Y., 2015. Petrogenesis of the similar to 2.77 Ga Monts de Cristal Complex, Gabon: Evidence for direct precipitation of Pt-arsenides from basaltic magma. *J. Petrol.* 56, 1285–1307.
- Mallick, D.I.J., Habgood, F., Skinner, A.C., 1981. A Geological Interpretation of LANDSAT Imagery and Air Photography of Botswana. HMSO, London.
- McCall, G.S., 2007. Behavioral ecological models of lithic technological change during the later Middle Stone Age of South Africa. *J. Archaeol. Sci.* 34, 1738–1751.

- McCarthy, T.S., Ellery, W.N., 1998. The Okavango Delta. *Trans. Royal Soc. South Africa* 53, 157–182.
- McCulloch, G.P., Irvine, K., Eckardt, F.D., Bryant, R.G., 2008. Hydrochemical fluctuations and crustacean community composition in an ephemeral saline lake (Sua Pan, Makgadikgadi Botswana). *Hydrobiologia* 596, 31–46.
- McFarlane, M.J., Eckardt, F.D., Ringrose, S., Coetzee, S.H., Kuhn, J.R., 2005. Degradation of linear dunes in northwest Ngamiland, Botswana and the implications for luminescence dating of periods of aridity. *Quat. Int.* 135, 83–90.
- Meltzer, D.J., 1989. Was stone exchanged among eastern North American paleo-Indians? In: Ellis, C.J., Lothrop, J.C. (Eds.), *Eastern Paleoindian Lithic Resource Use (Investigations in American Archaeology)*. Westview Press, Boulder, Colorado, pp. 11–39.
- Mendelsohn, J., 2022. The Angolan catchments of northern Botswana's major rivers: the Cubango, Cuito, Cuando and Zambezi rivers. In: Eckardt, F. (Ed.), *Landscapes and Landforms of Botswana*. Springer Nature, Heidelberg, pp. 15–36.
- Merrick, H.V., Brown, F.H., Nash, W.P., 1994. Use and movement of obsidian in the Early and Middle Stone Ages of Kenya and northern Tanzania. In: Childs, S.T. (Ed.), *Society, Culture, and Technology in Africa*. University of Pennsylvania Museum Applied Science Center for Archaeology, pp. 29–44.
- Middelburg, J.J., van der Weijden, C.H., Woittiez, J.R.W., 1988. Chemical processes affecting the mobility of major, minor and trace elements during weathering of granitic rocks. *Chem. Geol.* 68, 253–273.
- Miller, J.A., Harris, C., 2007. Petrogenesis of the Swaziland and northern Natal rhyolites of the Lebombo rifted volcanic margin, South East Africa. *J. Petrol.* 48, 185–218.
- Milzow, C., Kgotlhang, L., Bauer-Gottwein, P., Meier, P., Kinzelbach, W., 2009. Regional review: The hydrology of the Okavango Delta, Botswana - processes, data and modelling. *Hydrogeol. J.* 17, 1297–1328.
- Minichillo, T., 2006. Raw material use and behavioral modernity: Howiesons Poort lithic foraging strategies. *J. Hum. Evol.* 50, 359–364.
- Moore, A.E., Cotterill, F.P.D., Eckardt, F.D., 2012. The evolution and ages of Makgadikgadi palaeo-lakes: Consilient evidence from Kalahari drainage evolution in south-central Africa. *S. Afr. J. Geol.* 115, 385–413.
- Nash, D.J., 2022a. Dry valleys (mekgacha). In: Eckardt, F.D. (Ed.), *Landscapes and Landforms of Botswana*. Springer Nature, Heidelberg, pp. 179–199.
- Nash, D.J., 2022b. Calcretes, silcretes and intergrade duricrusts. In: Eckardt, F.D. (Ed.), *Landscapes and Landforms of Botswana*. Springer Nature, Heidelberg, pp. 223–246.
- Nash, D.J., Eckardt, F.D., 2016. Drainage development, neotectonics and base-level change in the Kalahari Desert, southern Africa. *S. Afr. Geogr. J.* 98, 308–320.
- Nash, D.J., Shaw, P.A., 1998. Silica and carbonate relationships in silcrete-calcrete intergrade duricrusts from the Kalahari of Botswana and Namibia. *J. Afr. Earth Sci.* 27, 11–25.
- Nash, D.J., Ulyott, J.S., 2007. Silcrete. In: Nash, D.J., McLaren, S.J. (Eds.), *Geochemical Sediments and Landscapes*. Blackwell, Oxford, pp. 95–143.
- Nash, D.J., McLaren, S.J., Webb, J.A., 2004. Petrology, geochemistry and environmental significance of silcrete-calcrete intergrade duricrusts at Kang Pan and Tswaane, Central Kalahari, Botswana. *Earth Surf. Process. Landforms* 29, 1559–1586.
- Nash, D.J., Coulson, S., Staurset, S., Ulyott, J.S., Babutsi, M., Hopkinson, L., Smith, M.P., 2013. Provenancing of silcrete raw materials indicates long-distance transport to Tsodilo Hills, Botswana, during the Middle Stone Age. *J. Hum. Evol.* 64, 280–288.
- Nash, D.J., Coulson, S., Staurset, S., Ulyott, J.S., Babutsi, M., Smith, M.P., 2016. Going the distance: Mapping mobility in the Kalahari Desert during the Middle Stone Age through multi-site geochemical provenancing of silcrete artefacts. *J. Hum. Evol.* 96, 113–133.
- Nash, D.J., Ciborowski, T.J.R., Ulyott, J.S., Parker Pearson, M., Darvill, T., Greaney, S., Maniatis, G., Whitaker, K.A., 2020. Origins of the sarsen megaliths at Stonehenge. *Sci. Adv.* 6, eabc0133. <https://doi.org/10.1126/sciadv.abc0133>.
- Neck, V., Kim, J.I., 2001. Solubility and hydrolysis of tetravalent actinides. *Radiochim. Acta* 89, 1–16.
- Nelson, M., 1991. The study of technological organization. *Archaeol. Method Theor.* 3, 57–100.
- Neumann, E.R., Svensen, H., Galerne, C.Y., Planke, S., 2011. Multistage evolution of dolerites in the Karoo Large Igneous Province, Central South Africa. *J. Petrol.* 52, 959–984.
- Oestmo, S., Schoville, B.J., Wilkins, J., Marean, C.W., 2014. A Middle Stone Age paleoscape near the Pinnacle Point caves, Vleesbaai, South Africa. *Quat. Int.* 350, 147–168.
- Olive, M., 2005. La perception du temps dans les sites magdaléniens de plein air du Bassin parisien. Du temps d'une occupation au temps des occupations. L'exemple du site d'Étiolles. *Bulletin de la Société préhistorique française*, pp. 763–770.
- Pastier, A.-M., Dauteuil, O., Murray-Hudson, M., Moreau, F., Walpersdorf, A., Makati, K., 2017. Is the Okavango Delta the terminus of the East African Rift System? Towards a new geodynamic model: Geodetic study and geophysical review. *Tectonophysics* 712–713, 469–481.
- Pearce, J.A., 1996. A user's guide to basalt discrimination diagrams. In: Wyman, D. (Ed.), *Trace Element Geochemistry of Volcanic Rocks: Application for Massive Sulphide Exploration*. Geological Association of Canada, Mineral Deposits Division, Winnipeg, pp. 79–113.
- Pelegriin, J., 1990. Prehistoric lithic technology: Some aspects of research. *Archaeol. Rev. Camb.* 9, 116–121.
- Porraz, G., Texier, P.-J., Archer, W., Piboule, M., Rigaud, J.-P., Tribolo, C., 2013. Technological successions in the Middle Stone Age sequence of Diepkloof rock shelter, Western Cape, South Africa. *J. Archaeol. Sci.* 40, 3376–3400.
- Richards, J.H., Burrough, S.L., Wiggs, G.F.S., Hills, T., Thomas, D.S.G., Moseki, M., 2021. Uneven surface moisture as a driver of dune formation on ephemeral lake beds under conditions similar to the present day: A model-based assessment from the Makgadikgadi Basin, northern Botswana. *Earth Surf. Process. Landforms* 46, 3078–3095.
- Ringrose, S., Huntsman-Mapila, P., Basira Kampunzu, A., Downey, W., Coetzee, S., Vink, B., Matheson, W., Vanderpost, C., 2005. Sedimentological and geochemical evidence for palaeo-environmental change in the Makgadikgadi subbasin, in relation to the MOZ rift depression, Botswana. *Palaeogeogr. Palaeoclimatol. Palaeoecol.* 217, 265–287.
- Ringrose, S., Harris, C., Huntsman-Mapila, P., Vink, B.W., Diskins, S., Vanderpost, C., Matheson, W., 2009. Origins of strandline duricrusts around the Makgadikgadi Pans (Botswana Kalahari) as deduced from their chemical and isotope composition. *Sediment. Geol.* 219, 262–279.
- Ringrose, S., Cassidy, L., Diskin, S., Coetzee, S., Matheson, W., Mackay, A.W., Harris, C., 2014. Diagenetic transformations and silcrete-calcrete intergrade duricrust formation in palaeo-estuary sediments. *Earth Surf. Process. Landforms* 39, 1167–1187.
- Robbins, L.H., Brook, G.A., Murphy, M.L., Campbell, A.C., Melear, N., Downey, W.S., 2000. Late Quaternary archaeological and palaeoenvironmental data from sediments at Rhino Cave, Tsodilo Hills, Botswana. *Southern African Field Archaeol.* 9, 17–31.
- Schmidt, M., Fuchs, M., Henderson, A.C.G., Kossler, A., Leng, M.J., Mackay, A.W., Shemang, E., 2017. Paleolimnological features of a mega-lake phase in the Makgadikgadi Basin (Kalahari, Botswana) during Marine Isotope Stage 5 inferred from diatoms. *J. Paleolimnol.* 58, 373–390.
- Shaw, P.A., Ames, C.J.H., Phillips, N., Chambers, S., Dosseto, A., Douglas, M., Goble, R., Jacobs, Z., Jones, B., Lin, S.C.-H., Low, M.A., McNeil, J.-L., Nasoordeen, S., O'Driscoll, C.A., Saktura, R.B., Sumner, T.A., Watson, S., Will, M., Mackay, A., 2019. The Doring River Archaeology Project: Approaching the evolution of human land use patterns in the Western Cape, South Africa. *PaleoAnthropology* 2019, 400–422.
- Shaw, P.A., Nash, D.J., 1998. Dual mechanisms for the formation of fluvial silcretes in the distal reaches of the Okavango Delta Fan, Botswana. *Earth Surf. Process. Landforms* 23, 705–714.
- Shaw, P.A., Cooke, H.J., Perry, C.C., 1990. Microbial silcretes in highly alkaline environments: Some observations from Sua Pan, Botswana. *S. Afr. J. Geol.* 93, 803–808.
- Shaw, P.A., Thomas, D.S.G., Nash, D.J., 1992. Late Quaternary fluvial activity in the dry valleys (mekgacha) of the Middle and Southern Kalahari, southern Africa. *J. Quat. Sci.* 7, 273–281.
- Shaw, P.A., Stokes, S., Thomas, D.S.G., Davies, F.B.M., Holmgren, K., 1997. Palaeoecology and age of a Quaternary high lake level in the Makgadikgadi Basin of the Middle Kalahari, Botswana. *South Afr. J. Sci.* 93, 273.
- Smith, R.A., 1984. The Lithostratigraphy of the Karoo Supergroup in Botswana (Bulletin 26). Botswana Geological Survey, Lobatse.
- Sossi, P.A., Eggins, S.M., Nesbitt, R.W., Nebel, O., Hergt, J.M., Campbell, I.H., O'Neill, H.S.C., Van Kranendonk, M., Davies, D.R., 2016. Petrogenesis and geochemistry of Archean komatiites. *J. Petrol.* 57, 147–184.
- Stadler, S., Osenbrück, K., Suckow, A.O., Himmelsbach, T., Hötzel, H., 2010. Ground-water flow regime, recharge and regional-scale solute transport in the semi-arid Kalahari of Botswana derived from isotope hydrology and hydrochemistry. *J. Hydrol.* 388, 291–303.
- Staurset, S., Coulson, S.D., Muthulathiphi, S., Burrough, S.L., Nash, D.J., Thomas, D.S.G., 2022a. Making points: The Middle Stone Age lithic industry of the Makgadikgadi Basin. Botswana. *Quat. Sci. Rev.* 107823. <https://doi.org/10.1016/j.quascirev.2022.107823>. In this issue.
- Staurset, S., Coulson, S.D., Muthulathiphi, S., Burrough, S.L., Nash, D.J., Thomas, D.S.G., 2022b. Post-depositional disturbance and spatial organization at exposed open-air sites: examples from the Middle Stone Age of the Makgadikgadi Basin. Botswana. *Quat. Sci. Rev.* 107824. <https://doi.org/10.1016/j.quascirev.2022.107824>. In this issue.
- Summerfield, M.A., 1982. Distribution, nature and genesis of silcrete in arid and semi-arid southern Africa. *Catena Suppl.* 1, 37–65.
- Summerfield, M.A., 1983. Silcrete. In: Goudie, A.S., Pye, K. (Eds.), *Chemical Sediments and Geomorphology*. Academic Press, London, pp. 59–91.
- Thiry, M., 1999. Diversity of continental silicification features: Examples from the Cenozoic deposits in the Paris Basin and neighbouring basement. In: Thiry, M., Simon-Coignou, R. (Eds.), *Palaeoweathering, Palaeosurfaces and Related Continental Deposits*. International Association of Sedimentologists, Special Publication No 27. Blackwell Science, Oxford, pp. 87–127.
- Thomas, D.S.G., Burrough, S.L., Coulson, S.D., Muthulathiphi, S., Nash, D.J., Staurset, S., 2022. Lacustrine geoarchaeology in the central Kalahari: Implications for Middle Stone Age behaviour and adaptation in dryland conditions. *Quat. Sci. Rev.* 107826. <https://doi.org/10.1016/j.quascirev.2022.107826>. In this issue.
- Thompson, E., Williams, H.M., Minichillo, T., 2010. Middle and late Pleistocene Middle Stone Age lithic technology from Pinnacle Point 13B (Mossel Bay, Western Cape province, South Africa). *J. Hum. Evol.* 59, 358–377.
- Turnbull, R.E., Alibone, A.H., Matheys, F., Fanning, C.M., Kasereka, E., Kabete, J., McNaughton, N.J., Mwandale, E., Holliday, J., 2021. Geology and geochronology of the Archean plutonic rocks in the northeast Democratic Republic of Congo. *Precambrian Res.* 358, 106133. <https://doi.org/10.1016/j.precamres.2021.106133>.

- Turunen, S.T., Luttinen, A.V., Heinonen, J.S., Jamal, D.L., 2019. Luenha picrites, Central Mozambique - messengers from a mantle plume source of Karoo continental flood basalts? *Lithos* 346, 105152. <https://doi.org/10.1016/j.lithos.2019.105152>.
- Wagner, L.J., Kleinhanns, I.C., Weber, N., Babechuk, M.G., Hofmann, A., Schoenberg, R., 2021. Coupled stable chromium and iron isotopic fractionation tracing magmatic mineral crystallization in Archean komatiite-tholeiite suites. *Chem. Geol.* 576, 120121. <https://doi.org/10.1016/j.chemgeo.2021.120121>.
- Webb, J.A., Nash, D.J., 2020. Reassessing southern African silcrete geochemistry: Implications for silcrete origin and sourcing of silcrete artefacts. *Earth Surf. Process. Landforms* 45, 3396–3413.
- White, K., Eckardt, F., 2006. Geochemical mapping of carbonate sediments in the Makgadikgadi basin, Botswana using moderate resolution remote sensing data. *Earth Surf. Process. Landforms* 31, 665–681.
- Wilkins, J., 2017. Middle Pleistocene lithic raw material foraging strategies at Kathu Pan 1, Northern Cape, South Africa. *J. Archaeol. Sci.: Report* 11, 169–188.
- Will, M., 2021. The role of different raw materials in lithic technology and settlement patterns during the Middle Stone Age of southern Africa. *Afr. Archaeol. Rev.* 38, 477–500.
- Will, M., Conard, N.J., 2020. Regional patterns of diachronic technological change in the Howiesons Poort of southern Africa. *PLoS ONE* 15, e0239195. <https://doi.org/10.1371/journal.pone.0239195>.
- Will, M., Parkington, J.E., Kandel, A.W., Conard, N.J., 2013. Coastal adaptations and the Middle Stone Age lithic assemblages from Hoedjiespunt 1 in the Western Cape, South Africa. *J. Hum. Evol.* 64, 518–537.
- Wilson, B.H., Dincer, T., 1976. An Introduction to the Hydrology and Hydrography of the Okavango Delta, Symposium on the Okavango Delta. Botswana Society, Gaborone, pp. 33–48.